In conclusion, anti-β2GPI was found to represent a risk factor for developing PIH in this case-controlled cohort study, providing evidence to support the utility of anti-β2GPI determination as one of the laboratory criteria for APS classification. In the previous SAPPORO prospective study, aPLs were measured during pregnancy and women with a history of recurrent spontaneous abortion or thrombosis who tested positive for lupus anticoagulant or aCL underwent low dose aspirin therapy. The knowledge of the presence of these aPLs could potentially influence the physician in favour of an early pregnancy termination. These possible biases can be excluded in the present case-controlled study. However, the subject number in our study is relatively small and furthermore we did not measure anti-β2GPI repeatedly 12 weeks apart, as required by the updated SAPPORO criteria (Miyakis et al., 2006). It is well known that aPLs share antigen epitopes and presence of one aPL increases the chance of the presence of the other aPLs. In women positive for anti-β2GPI but negative for lupus anticoagulant, aCL, phosphatidylserine-dependent anti-prothrombin antibody, or aPE, the presence of anti-β2GPI was not a significant risk factor for development of PIH or preeclampsia. This may partly be due to small numbers but it is also possible that an anti-β2GPI is only a marker for the presence of other more important aPLs. Larger studies designed to include appropriate adjustments for the presence of several aPLs should be undertaken to clarify this.

Acknowledgements

This work was supported in part by a Grant-in-Aid H20-kodomo-ippan-002 from the Ministry of Health, Labor and Welfare of Japan. We thank Dr. Hitoshi Okubo (The Sapporo Maternity Women's Hospital) for providing blood samples.

References

Ailus, K., Tulppala, M., Palosuo, T., Ylikorkala, O., Vaarala, O., 1996. Antibodies to beta 2-glycoprotein I and prothrombin in habitual abortion. Fertil. Steril. 66, 937–941.

Amengual, O., Atsumi, T., Khamashta, M., Koike, T., Hughes, G.R.V., 1996. Specificity of ELISA for antibody to beta2-glycoprotein I in patients with anti-phospholipid syndrome. Br. J. Rheumatol. 35, 1239–1243.

Arnold, J., Holmes, Z., Pickering, W., Farmer, C., Regan, L., Cohen, H., 2001. Anti-beta 2 glycoprotein 1 and anti-annexin V antibodies in women with recurrent miscarriage. Br. J. Haematol. 113, 911–914.

de Laat, B., Derksen, R.H., Urbanus, R.T., de Groot, P.G., 2004. IgG antibodies that recognize epitope Gly40-Arg43 in domain I of beta 2-glycoprotein I cause lupus anticoagulantC, and their presence correlates strongly with thrombosis. Blood 105, 1540–1545.

D'Ippolito, S., Di Simone, N., Di Nicuolo, F., Castellani, R., Caruso, A., 2007. Antiphospholipid antibodies: effects on trophoblast and endothelial cells. Am. J. Reprod. Immunol. 58, 150–158.

Di Simone, N., Raschi, E., Testoni, C., Castellani, R., D'Asta, M., Shi, T., Krilis, S.A., Caruso, A., Meroni, P.L., 2005. Pathogenic role of anti-beta 2-glycoprotein I antibodies in antiphospholipid associated fetal loss: characterisation of beta 2-glycoprotein I binding to trophoblast cells and functional effects of anti-beta 2-glycoprotein I antibodies in vitro. Ann. Rheum. Dis. 64, 462–467.

Di Simone, N., Meroni, P.L., D'Asta, M., Di Nicuolo, F., D'Alessio, M.C., Caruso, A., 2007. Pathogenic role of anti-beta2-glycoprotein I antibodies on human placenta: functional effects related to implantation and roles of heparin. Hum. Reprod. Update 13, 189–196.

Falcón, C.R., Martinuzzo, M.E., Forastiero, R.R., Cerrato, G.S., Carreras, L.O., 1997. Pregnancy loss and autoantibodies against phospholipid-binding proteins. Obstet. Gynecol. 89, 975–980.

Faden, D., Tincani, A., Tanzi, P., Spatola, L., Lojacono, A., Tarantini, M., Balestrieri, G., 1997. Anti-beta 2 glycoprotein I antibodies in a general obstetric population: preliminary results on the prevalence and correlation with pregnancy outcome. Anti-beta2 glycoprotein I antibodies are associated with some obstetrical complications, mainly preeclampsia–eclampsia. Eur. J. Obstet. Gynecol. Reprod. Biol. 73, 37–42.

Forastiero, R.R., Martinuzzo, M.E., Cerrato, G.S., Kordich, L.C., Carreras, L.O., 1997. Relationship of anti beta2-glycoprotein I and anti prothrombin antibodies to thrombosis and pregnancy loss in patients with antiphospholipid antibodies. Thromb. Haemost. 78, 1008–1014.

Hulstein, J.J., Lenting, P.J., de Laat, B., Derksen, R.H., Fijnheer, R., de Groot, P.G., 2007. beta2-Glycoprotein I inhibits von Willebrand factor dependent platelet adhesion and aggregation. Blood 110, 1483–1491.

Lee, R.M., Emlen, W., Scott, J.R., Branch, D.W., Silver, R.M., 1999. Anti-beta2-glycoprotein I antibodies in women with recurrent spontaneous abortion, unexplained fetal death, and antiphospholipid syndrome. Am. J. Obstet. Gynecol. 181, 642–648.

Lee, R.M., Brown, M.A., Branch, D.W., Ward, K., Silver, R.M., 2003. Anticardiolipin and anti-beta2-glycoprotein-I antibodies in preeclampsia. Obstet. Gynecol. 102, 294–300.

Lynch, A., Byers, T., Emlen, W., Rynes, D., Shetterly, S.M., Hamman, R.F., 1999. Association of antibodies to beta2-glycoprotein 1 with pregnancy loss and pregnancy-induced hypertension: a prospective study in low-risk pregnancy. Obstet. Gynecol. 93, 193–198.

Martinuzzo, M.E., Forastiero, R.R., Carreras, L.O., 1995. Anti beta 2 glycoprotein I antibodies: detection and association with thrombosis. Br. J. Haematol. 89, 397–402.

Miyakis, S., Lockshin, M.D., Atsumi, T., Branch, D.W., Brey, R.L., Cervera, R., Derksen, R.H., Groot, D.E., Koike, P.G., Meroni, T., Reber, P.L., Shoenfeld, G., Tincani, Y., Vlachoyiannopoulos, A., Krilis, P.G., S.A., 2006. International consensus statement on an update of the classification criteria for definite antiphospholipid syndrome (APS). J. Thromb. Haemost. 4, 295–306.

Pengo, V., Biasiolo, A., Pegoraro, C., Cucchini, U., Noventa, F., Iliceto, S., 2005. Antibody profiles for the diagnosis of antiphospholipid syndrome. Thromb. Haemost. 93, 1147–1152.

Sailer, T., Zoghlami, C., Kurz, C., Rumpold, H., Quehenberger, P., Panzer, S., Pabinger, I., 2006. Anti-beta2-glycoprotein I antibodies are associated with pregnancy loss in women with the lupus anticoagulant. Thromb. Haemost. 95, 796–801.

Sanmarco, M., Gayet, S., Alessi, M.C., Audrain, M., de Maistre, E., Gris, J.C., de Groot, P.G., Hachulla, E., Harlé, J.R., Sié, P., Boffa, M.C., 2007. Antiphosphatidylethanolamine antibodies are associated with an increased odds ratio for thrombosis. Thromb. Haemost. 97, 949–954.

Stern, C., Chamley, L., Hale, L., Kloss, M., Speirs, A., Baker, H.W., 1998. Antibodies to beta2 glycoprotein I are associated with in vitro fertilization implantation failure as well as recurrent miscarriage: results of a prevalence study. Fertil. Steril. 70, 938–944.

Wilson, W.A., Gharavi, A.E., Koike, T., Lockshin, M.D., Branch, D.W., Piette, J.C., Brey, R., Derksen, R., Harris, E.N., Hughes, G.R., Triplett, D.A., Khamashta, M.A., 1999. International consensus statement on preliminary classification criteria for definite antiphospholipid syndrome: report of an international workshop. Arthritis Rheum. 42, 1309–1311.

Yamada, H., Atsumi, T., Kobashi, G., Ota, C., Kato, E.H., Tsuruga, N., Ohta, K., Yasuda, S., Koike, T., Minakami, H., 2009. Antiphospholipid antibodies increase the risk of pregnancy-induced hypertension and adverse pregnancy outcomes. J. Reprod. Immunol. 79, 188–195.

Zanon, E., Prandoni, P., Vianello, F., Saggiorato, G., Carraro, G., Bagatella, P., Girolami, A., 1999. Anti-beta2-glycoprotein I antibodies in patients with acute venous thromboembolism: prevalence and association with recurrent thromboembolism. Thromb. Res. 96, 269–274.

Zoghlami-Rintelen, C., Vormittag, R., Sailer, T., Lehr, S., Quehenberger, P., Rumpold, H., Male, C., Pabinger, I., 2005. The presence of IgG antibodies against beta2-glycoprotein I predicts the risk of thrombosis in patients with the lupus anticoagulant. J. Thromb. Haemost. 3, 1160–1165.

ARTHRITIS & RHEUMATISM
Vol. 62, No. 2, February 2010, pp 574–579
DOI 10.1002/art.27190

The Association of a Nonsynonymous Single-Nucleotide Polymorphism in *TNFAIP3* With Systemic Lupus Erythematosus and Rheumatoid Arthritis in the Japanese Population

Kenichi Shimane,[1] Yuta Kochi,[2] Tetsuya Horita,[3] Katsunori Ikari,[4] Hirofumi Amano,[5] Michito Hirakata,[6] Akiko Okamoto,[7] Ryo Yamada,[8] Keiko Myouzen,[2] Akari Suzuki,[2] Michiaki Kubo,[2] Tatsuya Atsumi,[3] Takao Koike,[3] Yoshinari Takasaki,[5] Shigeki Momohara,[4] Hisashi Yamanaka,[4] Yusuke Nakamura,[8] and Kazuhiko Yamamoto[1]

Objective. **Genome-wide association (GWA) studies in systemic lupus erythematosus (SLE) and rheumatoid arthritis (RA) in Caucasian populations have independently identified risk variants in and near the tumor necrosis factor α (TNFα)–induced protein 3 gene (*TNFAIP3*), which is crucial for the regulation of TNF-mediated signaling and Toll-like receptor signaling. The aim of this study was to assess the role of *TNFAIP3* in the development of SLE and RA in Japanese subjects.**

Methods. **We selected 2 single-nucleotide polymorphisms (SNPs) from previous GWA studies. Rs2230926 is a nonsynonymous SNP in *TNFAIP3* and is associated with SLE, while rs10499194 is an intergenic SNP associated with RA. We then performed 2 independent sets of SLE case–control comparisons (717 patients and 1,362 control subjects) and 3 sets of RA case–control comparisons (3,446 patients and 2,344 control subjects) using Japanese subjects. We genotyped SNPs using TaqMan assays.**

Results. **We observed a significant association between rs2230926 and an increased risk of SLE and RA in the Japanese population (for SLE, odds ratio [OR] 1.92, 95% confidence interval [95% CI] 1.53–2.41, $P = 1.9 \times 10^{-8}$; for RA, OR 1.35, 95% CI 1.18–1.56, $P = 2.6 \times 10^{-5}$). The intergenic SNP rs10499194 was also associated with SLE and RA, while the risk allele for RA in Caucasians was protective against the diseases in our population.**

Drs. Shimane, Kochi, Yamada, Myouzen, Suzuki, Kubo, Nakamura, and Yamamoto's work was supported by a grant from the Center for Genomic Medicine (CGM), Institute of Physical and Chemical Research (RIKEN). Drs. Horita, Amano, Hirakata, Okamoto, Yamada, Atsumi, Koike, and Takasaki's work was supported by a grant from the Japanese Ministry of Health, Labor, and Welfare. Drs. Ikari, Momohara, and Yamanaka's work was supported by a Japan Orthopaedics and Traumatology Foundation grant, a Takeda Science Foundation grant, and a Japanese Ministry of Education, Culture, Sports, Science, and Technology grant-in-aid for scientific research. The Institute of Rheumatology Rheumatoid Arthritis cohort was supported by 36 pharmaceutical companies.

[1]Kenichi Shimane, MD, PhD, Kazuhiko Yamamoto, MD, PhD: Graduate School of Medicine, University of Tokyo, Tokyo, Japan, and CGM, RIKEN, Yokohama, Japan; [2]Yuta Kochi, MD, PhD, Keiko Myouzen, MSc, Akari Suzuki, PhD, Michiaki Kubo, MD, PhD: CGM, RIKEN, Yokohama, Japan; [3]Tetsuya Horita, MD, PhD, Tatsuya Atsumi, MD, PhD, Takao Koike, MD, PhD: Hokkaido University Graduate School of Medicine, Sapporo, Japan; [4]Katsunori Ikari, MD, PhD, Shigeki Momohara, MD, PhD, Hisashi Yamanaka, MD, PhD: Tokyo Women's Medical University, Tokyo, Japan; [5]Hirofumi Amano, MD, PhD, Yoshinari Takasaki, MD, PhD: School of Medicine, Juntendo University, Tokyo, Japan; [6]Michito Hirakata, MD, PhD: Keio University School of Medicine, Tokyo, Japan; [7]Akiko Okamoto, MD, PhD: Graduate School of Medicine, University of Tokyo, Tokyo, Japan; [8]Ryo Yamada, MD, PhD, Yusuke Nakamura, MD, PhD: Institute of Medical Science, University of Tokyo, Tokyo, Japan.

Dr. Ikari has received speaking fees from Abbott Japan and Mitsubishi Tanabe Pharma (less than $10,000 each). Dr. Momohara has received speaking fees from Astellas Pharma, Chugai Pharmaceutical, Dainippon Sumitomo Pharma, Kaken Pharmaceutical, Mitsubishi Tanabe Pharma, Sanofi-Aventis, Santen Pharmaceutical, Takeda Pharmaceutical, and Wyeth (less than $10,000 each). Dr. Yamanaka has received speaking fees from Abbott Japan, Chugai Pharmaceutical, Eisai, Mitsubishi Tanabe Pharma, Hoffman-LaRoche, Takeda Pharmaceutical, and Wyeth (less than $10,000 each). Dr. Yamamoto has received consulting fees, speaking fees, or honoraria from Astellas Pharma and Chugai Pharmaceutical (less than $10,000 each) and owns stock or stock options in ImmunoFuture.

Address correspondence and reprint requests to Yuta Kochi, MD, PhD, Laboratory for Autoimmune Diseases, CGM, RIKEN, 7-3-1 Hongo, Bunkyo-Ku, Tokyo 113-0033, Japan. E-mail: ykochi@src.riken.jp.

Submitted for publication May 6, 2009; accepted in revised form October 2, 2009.

Conclusion. **We demonstrated a significant association between the nonsynonymous variant in *TNFAIP3* and the risk for SLE and RA in the Japanese population. *TNFAIP3*, similar to *STAT4* and *IRF5*, may be a common genetic risk factor for SLE and RA that is shared between the Caucasian and Japanese populations.**

Systemic lupus erythematosus (SLE) and rheumatoid arthritis (RA) represent multigenic diseases and are considered to be caused by interactions between susceptibility genes and environmental factors that result in an abnormal immune response. In fact, familial and linkage studies have provided strong evidence for the role of multiple genetic factors in the development of SLE and RA (1). In addition, association-based approaches in candidate loci using single-nucleotide polymorphisms (SNPs) have also identified several genes that contribute to these diseases. More recently, genome-wide association (GWA) studies in SLE and RA have revealed many susceptibility genes and pathways that contribute to disease development (2).

Familial and linkage studies have also shown familial aggregation of RA, SLE, and other immune-mediated diseases (1). In fact, several gene polymorphisms, including *PTPN22*, *STAT4,* and *IRF5* variants, have been shown to predispose to SLE and RA. Recent GWA studies in Caucasian populations have also identified the tumor necrosis factor α (TNFα)–induced protein 3 gene (*TNFAIP3*) as another common genetic risk factor for SLE and RA (3–6). *TNFAIP3*, also known as the A20 protein, is a negative regulator of the NF-κB signaling pathway that is essential in the pathogenesis of both SLE and RA (7). The association of *TNFAIP3* with diseases has been independently reported in SLE and RA, and it is of great interest that the peaks in association in the GWA studies are different between SLE and RA. In Caucasian populations, the significantly associated SNP markers for SLE, including the nonsynonymous SNP termed rs2230926, are located in the *TNFAIP3* region, while those for RA are located in the intergenic region between *TNFAIP3* and the oligodendrocyte transcription factor 3 gene (*OLIG3*). In addition to the difference in the diseases themselves, the association between *TNFAIP3* polymorphisms and these diseases in the Asian populations remains unclear (8).

In order to elucidate a genetic role for *TNFAIP3* in the development of SLE and RA in the Japanese population, we investigated 2 independent case–control cohorts of patients with SLE and 3 independent cohorts of patients with RA.

PATIENTS AND METHODS

Subjects. The subjects in the SLE study group comprised 2 cohorts of Japanese patients with SLE and unrelated control subjects. An SLE case–control cohort from the RIKEN (SLE cohort 1) consisted of 376 patients (mean age 43.2 years, 90.3% women) and 934 unrelated control subjects (mean age 52.6 years, 25.0% women). An SLE case–control cohort at Hokkaido University (SLE cohort 2) consisted of 341 patients (mean age 46.2 years, 88.3% women) and 428 unrelated control subjects (mean age 47.7 years, 28.7% female). All patients with SLE fulfilled the 1997 American College of Rheumatology (ACR) revised criteria for SLE (9).

The subjects in the RA component of the study comprised 3 cohorts of Japanese patients with RA and unrelated control subjects. The first cohort of patients with RA from BioBank Japan (RA cohort 1) consisted of 1,112 patients (mean age 60.5 years, 89.7% female, 69.7% positive for rheumatoid factor [RF]), and 934 unrelated control subjects. The second cohort from RIKEN (RA cohort 2) consisted of 830 patients (mean age 64.3 years, 83.7% women, 75.0% RF positive), and 658 unrelated control subjects (mean age 48.6 years, 57.4% women). The 934 unrelated control subjects in the first cohort of RA patients were the same as those used in SLE cohort 1. An RA case–control cohort from the Institute of Rheumatology Rheumatoid Arthritis (IORRA) cohort (RA cohort 3), which is a prospective observational cohort of patients with RA studied at Tokyo Women's Medical University, comprised 1,504 patients (mean age 59.3 years, 84% women, 88% RF positive), and 752 control subjects (mean age 38.4 years, 50% women). All patients with RA met the 1987 ACR (formerly, the American Rheumatism Association) revised criteria for a diagnosis of RA (10).

All subjects entered into this study were self-identified as Japanese and were recruited through several medical institutions located in Japan. DNA samples from the patients in the first cohort of RA patients in BioBank Japan were provided by the Leading Project for Personalized Medicine from the Ministry of Education, Culture, Sports, Science and Technology, Japan (11). All subjects provided informed consent prior to their participation in this study, and the study was preapproved by the ethics committee of each institution.

SNPs. For the selection of SNPs required to genotype in and near *TNFAIP3*, we reviewed previous GWA studies of SLE and RA (3–6). We then selected 2 SNPs, rs2230926 and rs10499194. SNP rs2230926 is a nonsynonymous variant in exon 3 of *TNFAIP3* and was strongly associated with SLE in the GWA study by Musone et al (5). Although the GWA study of SLE by Graham et al indicated that rs5029939, located in intron 2 of the gene, is most significantly associated with a predisposition to SLE (6), there is strong linkage disequilibrium (LD) ($r^2 = 0.86$) between these SNPs according to HapMap phase II data for Japanese and evidence that rs5029939 may be substituted by rs2230926 (Figure 1). Two previous GWA studies in RA revealed that rs10499194 and rs6920220, which are located between *TNFAIP3* and *OLIG3*, were significantly associated risk variants for RA (3,4). The HapMap data for Japanese individuals indicate that the minor allele frequency (MAF) of rs6920220 is 0.011, and that the MAF for control subjects in RA cohort 3 (IORRA) was <0.01. Results of a recent study in Korean populations also indicated

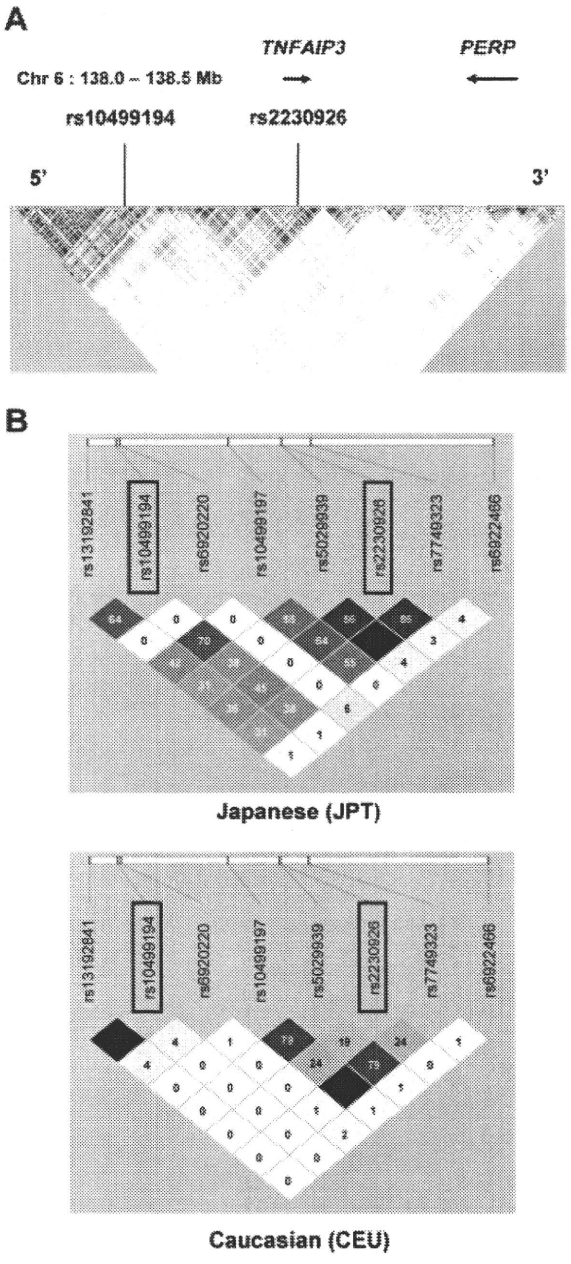

Figure 1. Pairwise linkage disequilibrium (LD) patterns for polymorphisms in the *TNFAIP3* region, according to HapMap phase II data. **A,** Pairwise LD pattern in the expanded *TNFAIP3* region derived from the HapMap data for Japanese patients, with r^2 values. *OLIG3* is located ~370 kbp away from *TNFAIP3* in the 5′ region and is not shown. **B,** Pairwise LD patterns for single-nucleotide polymorphisms (SNPs) in the *TNFAIP3* region that were significantly associated with systemic lupus erythematosus and rheumatoid arthritis in previous genome-wide association studies. The upper and lower panels were constructed using HapMap data for Japanese and Caucasian patients, respectively. The diagram shows pairwise LD values as quantified using the r^2 value. A stronger LD is depicted graphically by the densely shaded boxes. The boxed areas show the 2 SNPs genotyped.

that the variant was too rare (MAF <0.01) to be evaluated for associations (8).

Based on HapMap data for Japanese individuals, pairwise LD patterns for the SNPs in and near *TNFAIP3*, which were significantly associated with SLE and RA in the previous GWA studies, are presented in Figure 1 (for SLE, rs13192841, rs10499197, rs5029939, rs2230926, rs7749323, and rs6922466; for RA, rs10499194 and rs6920220).

Genotyping. We genotyped SNPs using TaqMan assays. For the selected SNPs, predesigned TaqMan SNP genotyping assays were used (probe ID: rs2230926, C.770116_10; rs10499194, C.1575581_10; Applied Biosystems, Foster City, CA). Fluorescence was detected using an ABI Prism 7900HT Sequence Detection System (Applied Biosystems). Genotyping assessment was performed on >98% of the samples, for all of the polymorphisms genotyped. All of the SNPs were in Hardy-Weinberg equilibrium in control subjects, according to chi-square statistics ($P > 0.01$).

Case–control association tests. We first performed allele frequency comparisons of rs2230926 and rs10499194 in SLE cohort 1 and RA cohort 1. Then, further case–control association studies were conducted using SLE cohort 2 and RA cohorts 2 and 3, to validate the associations in the first cohorts. In the replication studies, we genotyped the SNPs with a P value less than 0.05 in either SLE cohort 1 or RA cohort 1 (the P value was determined after correction for conditional logistic analysis, as described below).

Measurement of autoantibodies. Sera from 1,104 patients in RA cohort 1 were available for the measurement of anti–cyclic citrullinated peptide (anti-CCP) antibodies and RF. Anti-CCP antibodies were measured using the Mesacup CCP test (Medical and Biological Laboratories, Woburn, MA), and RF was measured by enzyme-linked immunosorbent assay.

Statistical analysis. The case–control association of each SNP was tested with the Cochran-Armitage trend test. The genotype and allele frequencies for patients and control subjects were used to calculate the odds ratios (ORs) and 95% confidence interval (95% CIs) using Woolf's method. For the combined analysis, we used the Mantel-Haenszel test. We performed conditional logistic regression analysis to evaluate the effect of each polymorphism conditional on the remaining polymorphisms, using Statistica software (StatSoft, Tulsa, OK). We calculated pairwise LD indices between pairs of SNPs (the r^2 value), using HaploView software, version 4.0 (http://www.broad.mit.edu/haploview/ haploview). We calculated the population attributable risk (PAR) using the following formula: $PAR = f(OR - 1)/(1 + f[OR - 1])$, where f is the allele frequency in the control subjects. PAR is defined as the reduction in incidence that would be achieved if the population had been entirely unexposed. We calculated the statistical power of association using the R software program (http://www.r-project.org).

RESULTS

Our results revealed a significant association between rs2230926 and both SLE and RA when comparing allele frequency in the patients and control subjects in the first cohort (for SLE, OR 1.92, 95% CI

Table 1. Association study of rs2230926 and rs10499194 with SLE in Japanese subjects*

dbSNP number, major/minor allele	No. of patients	No. of controls	Minor allele frequency		OR (95% CI)	*P*
			Patients	Controls		
rs2230926, G/T						
SLE 1	376	934	0.113	0.062	1.92 (1.43–2.58)	1.2×10^{-5}
SLE 2	341	428	0.116	0.064	1.91 (1.33–2.73)	3.0×10^{-4}
Combined analysis†	717	1,362	0.114	0.063	1.92 (1.53–2.41)	1.9×10^{-8}
rs10499194, T/C						
SLE 1	376	933	0.084	0.061	1.42 (1.03–1.95)	0.030

* SLE = systemic lupus erythematosus; dbSNP = Database of Single-Nucleotide Polymorphisms; OR = odds ratio; 95% CI = 95% confidence interval.
† By the Mantel-Haenszel method.

1.43–2.58, $P = 1.2 \times 10^{-5}$; for RA, OR 1.52, 95% CI 1.20–1.92, $P = 5.6 \times 10^{-4}$) (Tables 1 and 2). We also observed an association between rs10499194 and SLE patients in cohort 1 (OR 1.42, 95% CI 1.03–1.95, $P = 0.030$) (Table 1). However, the T allele appeared to represent a susceptibility allele in the SLE and RA patients in cohort 1, whereas the C allele appeared to be a risk allele for RA in Caucasians (3). We speculated that this association could be secondary to the moderate LD between rs2230926 and rs10499194 ($r^2 = 0.14$) according to data on control subjects in SLE cohort 1, and we subsequently performed a conditional logistic regression analysis to evaluate the effects of each polymorphism conditional on the remaining polymorphisms. The results of this analysis indicated that rs10499194 did not retain the statistically significant association when conditionally evaluated on rs2230926 ($P = 0.73$), while rs2230926 retained the significant association when conditionally evaluated on rs10499194 ($P = 3.4 \times 10^{-4}$). We concluded that rs2230926 was primarily associated with SLE located at this locus, and therefore genotyped only rs2230926 for replication studies in SLE (3–6).

The results of a case–control association study in SLE cohort 2 confirmed the significant association between rs2230926 and the risk of SLE (OR 1.91, 95% CI 1.33–2.73, $P = 3.0 \times 10^{-4}$). A combined analysis also confirmed a significant association (OR 1.92, 95% CI 1.53–2.41, $P = 1.9 \times 10^{-8}$, PAR = 0.055). In RA cohort 2 a statistically significant association between rs2230926 and a predisposition for RA was also replicated; however, this was not replicated in RA cohort 3 (for cohort 2, OR 1.39, 95% CI 1.07–1.81, $P = 0.013$; for cohort 3, OR 1.19, 95% CI 0.94–1.50, $P = 0.15$) (Table 2). In RA cohort 3, the statistical power required to detect an association at rs2230926 was 0.54 at a significance level of $\alpha = 0.05$ when we presumed that the OR for RA was 1.4 (the combined OR for RA cohorts 1 and 2 was 1.46). It was possible that the statistical power for RA cohort 3 may have been insufficient. A combined analysis on these data suggested a significant association (OR 1.35, 95% CI 1.18–1.56, $P = 2.6 \times 10^{-5}$, PAR = 0.024).

We observed no significant association of rs10499194 in RA cohort 1, but the statistical power to detect the association in this study was insufficient (1 −

Table 2. Association study of rs2230926 and rs10499194 with RA in Japanese subjects*

dbSNP number, minor/major allele	No. of Patients	No. of controls	Minor allele frequency		OR (95% CI)	*P*
			Patients	Controls		
rs2230926, G/T						
RA cohort 1	1,112	934	0.091	0.062	1.52 (1.20–1.92)	5.6×10^{-4}
RA cohort 2	825	655	0.100	0.074	1.39 (1.07–1.81)	0.013
RA cohort 3	1,478	747	0.087	0.075	1.19 (0.94–1.50)	0.15
Combined analysis†	3,415	2,326	0.092	0.069	1.35 (1.18–1.56)	2.6×10^{-5}
rs10499194, T/C						0.26
RA cohort 1	1,112	933	0.069	0.061	1.15 (0.90–1.48)	0.26
RA cohort 2	827	650	0.072	0.048	1.52 (1.11–2.08)	0.0090
RA cohort 3	1,472	716	0.073	0.059	1.32 (1.02–1.73)	0.038
Combined analysis†	3,411	2,299	0.071	0.056	1.30 (1.11–1.53)	8.4×10^{-4}

* RA = rheumatoid arthritis; dsSNP = Database of Single-Nucleotide Polymorphisms; OR = odds ratio; 95% CI = 95% confidence interval.
† By the Mantel-Haenszel method.

$\beta = 0.31$) considering the previously reported OR of 0.75 and a significance level of $\alpha = 0.05$ (3). Therefore, we genotyped rs10499194 in RA cohorts 2 and 3 for confirmation. Unlike in RA cohort 1, a significant association of rs10499194 was observed in RA cohorts 2 and 3 (for cohort 2, OR 1.52, 95% CI 1.11–2.08, $P = 0.0090$; for cohort 3, OR 1.32, 95% CI 1.02–1.73, $P = 0.038$) (Table 2). However, the risk allele for Caucasian patients with RA was protective against RA in our population, just as was observed in SLE cohort 1. The combined analysis showed a significant association of rs10499194 with RA (OR 1.30, 95% CI 1.11–1.53, $P = 8.4 \times 10^{-4}$).

We stratified patients in RA cohorts 1 and 3 according to the presence of anti-CCP antibodies and RF and examined for the association between *TNFAIP3* polymorphisms (rs2230926 and rs10499194) and RA susceptibility (see Supplementary Table 1, available in the online version of this article at http://www3.interscience.wiley.com/journal/76509746/home). When the patients were stratified according to anti-CCP antibody status, the G allele of rs2230926 was found to confer increased risk for RA in anti-CCP antibody–positive patients relative to anti-CCP antibody–negative patients (for anti-CCP antibody–positive patients, OR 1.36, 95% CI 1.15–1.62, $P = 4.0 \times 10^{-4}$; for anti-CCP–negative patients, OR 1.16, 95% CI 0.83–1.61, $P = 0.39$ in the combined analysis). A similar trend was observed when patients were stratified according to RF status. A stratified analysis on rs10499194 also showed that the disease susceptibility allele in Japanese patients with RA (the T allele) conferred higher risk in autoantibody-positive patients than in autoantibody-negative patients.

DISCUSSION

In the current study, rs2230926, located in exon 3 of *TNFAIP3,* was shown to be significantly associated with a predisposition to both SLE and RA in 2 and 3 independent cohorts of subjects, respectively. Our results confirmed that *TNFAIP3* is one of the common genetic risk factors for both SLE and RA, similar to *STAT4* and *IRF5*, in the Japanese and Caucasian populations (2). In addition, recent studies in Caucasian patients with RA have demonstrated that the *TNFAIP3* variant conferred an increased risk of RA in anti-CCP antibody– and RF-positive patients compared with anti-CCP antibody– and RF-negative patients (12,13). Our analysis stratified according to the autoantibodies confirmed this observation in Japanese patients with RA.

TNFAIP3 encodes a cytoplasmic zinc finger protein that is also known as the A20 protein. The A20 protein is required for negative regulation of the NF-κB signaling pathway, which is mediated by innate immune receptors such as TNF receptors and Toll-like receptors, and it prevents overstimulation of the innate immune response (7,14). The disease-associated variant, rs2230926 (T/G), is a nonsynonymous variant that results in a phenylalanine-to-cysteine change at residue 127 of the A20 protein (5). The risk allele is known to be the G allele that encodes Cys. Musone et al have reported that Cys^{127} A20 protein was only modestly, but consistently, less effective at inhibiting TNF-induced NF-κB activity than the Phe^{127} protein (5). This result suggests that reduced negative regulatory activity of A20 protein may allow excessive immune activity, leading to enhanced autoreactivity.

GWA studies of SLE patients in Caucasian populations have suggested that several polymorphisms in the *TNFAIP3* region, including the nonsynonymous SNP rs2230926, are associated with a predisposition to the disease. The genetic significance of rs2230926 was evident in the Japanese patients with SLE or RA entered into our study, although its precise role in Caucasian patients with RA remains unclear. The intergenic SNP rs10499194 is one of the landmark polymorphisms identified in Caucasian patients with RA (3,15), although the significant association with RA could not be replicated in several Caucasian populations (3,12). Because rs10499194 is also associated with RA susceptibility and autoantibody status in our population, rs10499194 could be a landmark for disease causal variants in Japanese patients with RA. However, considering the inverted susceptibility allele of rs10499194 between Japanese patients (T allele) and Caucasian patients (C allele), this association of rs10499194 would appear to be secondary, as a result of LD between rs10499194 and the disease causal variants. This finding is further supported by the lack of independent association at rs10499194 in SLE when conditioned with the rs2230926 genotype, suggesting that the association observed in rs10499194 may be partially influenced by rs2230926.

Taking into account the biologic impact of rs2230926 demonstrated by Musone et al (5), rs2230926 seems likely to be an important candidate for a causal variant in *TNFAIP3* (5). However, additional polymorphisms that are located in the intergenic region of *OLIG3* and *TNFAIP3* as well as that of *TNFAIP3* and *PERP* may also independently exercise an effect on disease susceptibility, a hypothesis that was previously raised by Musone et al (5) and Graham et al (6). Further mapping of the *TNFAIP3* region in Asian and Caucasian

populations is required for the precise determination of the additional causal polymorphisms present in patients with RA or SLE.

In conclusion, we confirm that *TNFAIP3* is a genetic risk factor for the development of both SLE and RA in the Japanese population. Although the nonsynonymous SNP rs2230926 is a strong causal variant candidate in this region, a search for additional causal variants in *TNFAIP3* is required.

ACKNOWLEDGMENTS

We are grateful to Drs. M. Yukioka, S. Tohma, Y. Nishioka, T. Matsubara, S. Wakitani, R. Teshima, and T. Sawada for their dedication in referring patients to the study and for clinical sample collection. We also thank Dr. A. Miyatake, the members of the Rotary Club of Osaka-Midosuji District 2660 Rotary International in Japan, and the staff of the BioBank Japan Project for supporting both the study and the clinical sample collection. We thank Dr. S. Tsukahara of the IORRA study and all members of the Laboratory for Autoimmune Diseases, CGM, RIKEN, for their helpful advice and excellent technical assistance.

AUTHOR CONTRIBUTIONS

All authors were involved in drafting the article or revising it critically for important intellectual content, and all authors approved the final version to be published. Dr. Kochi had full access to all of the data in the study and takes responsibility for the integrity of the data and the accuracy of the data analysis.

Study conception and design. Shimane, Kochi, Horita, Ikari, Yamada, Atsumi, Koike, Momohara, Yamanaka, Nakamura, Yamamoto.

Acquisition of data. Shimane, Kochi, Horita, Ikari, Amano, Hirakata, Okamoto, Myouzen, Suzuki, Kubo, Takasaki.

Analysis and interpretation of data. Shimane, Kochi, Horita, Ikari, Yamamoto.

REFERENCES

1. Alarcon-Segovia D, Alarcon-Riquelme ME, Cardiel MH, Caeiro F, Massardo L, Villa AR, et al. Familial aggregation of systemic lupus erythematosus, rheumatoid arthritis, and other autoimmune diseases in 1,177 lupus patients from the GLADEL cohort. Arthritis Rheum 2005;52:1138–47.
2. Gregersen PK, Olsson LM. Recent advances in the genetics of autoimmune disease. Annu Rev Immunol 2009;27:363–91.
3. Plenge RM, Cotsapas C, Davies L, Price AL, de Bakker PI, Maller J, et al. Two independent alleles at 6q23 associated with risk of rheumatoid arthritis. Nat Genet 2007;39:1477–82.
4. Thomson W, Barton A, Ke X, Eyre S, Hinks A, Bowes J, et al. Rheumatoid arthritis association at 6q23. Nat Genet 2007;39: 1431–3.
5. Musone SL, Taylor KE, Lu TT, Nititham J, Ferreira RC, Ortmann W, et al. Multiple polymorphisms in the TNFAIP3 region are independently associated with systemic lupus erythematosus. Nat Genet 2008;40:1062–4.
6. Graham RR, Cotsapas C, Davies L, Hackett R, Lessard CJ, Leon JM, et al. Genetic variants near TNFAIP3 on 6q23 are associated with systemic lupus erythematosus. Nat Genet 2008;40:1059–61.
7. Lee EG, Boone DL, Chai S, Libby SL, Chien M, Lodolce JP, et al. Failure to regulate TNF-induced NF-κB and cell death responses in A20-deficient mice. Science 2000;289:2350–4.
8. Lee HS, Korman BD, Le JM, Kastner DL, Remmers EF, Gregersen PK, et al. Genetic risk factors for rheumatoid arthritis differ in caucasian and Korean populations. Arthritis Rheum 2009;60: 364–71.
9. Hochberg MC, for the Diagnostic and Therapeutic Criteria Committee of the American College of Rheumatology. Updating the American College of Rheumatology revised criteria for the classification of systemic lupus erythematosus [letter]. Arthritis Rheum 1997;40:1725.
10. Arnett FC, Edworthy SM, Bloch DA, McShane DJ, Fries JF, Cooper NS, et al. The American Rheumatism Association 1987 revised criteria for the classification of rheumatoid arthritis. Arthritis Rheum 1988;31:315–24.
11. Nakamura Y. The BioBank Japan Project. Clin Adv Hematol Oncol 2007;5:696–7.
12. Perdigones N, Lamas JR, Vigo AG, de la Concha EG, Jover JA, Urcelay E, et al. 6q23 polymorphisms in rheumatoid arthritis Spanish patients. Rheumatology (Oxford) 2009;48:618–21.
13. Patsopoulos NA, Ioannidis JP. Susceptibility variants for rheumatoid arthritis in the TRAF1-C5 and 6q23 loci: a meta-analysis. Ann Rheum Dis 2009. E-pub ahead of print.
14. Liu YC, Penninger J, Karin M. Immunity by ubiquitylation: a reversible process of modification. Nat Rev Immunol 2005;5: 941–52.
15. Orozco G, Hinks A, Eyre S, Ke X, Gibbons LJ, Bowes J, et al. Combined effects of three independent SNPs greatly increase the risk estimate for RA at 6q23. Hum Mol Genet 2009;18:2693–9.

Arthritis Care & Research
Vol. 62, No. 5, May 2010, pp 657–663
DOI 10.1002/acr.20110

ORIGINAL ARTICLE

Change of Synovial Vascularity in a Single Finger Joint Assessed by Power Doppler Sonography Correlated With Radiographic Change in Rheumatoid Arthritis: Comparative Study of a Novel Quantitative Score With a Semiquantitative Score

JUN FUKAE,[1] YUJIRO KON,[1] MIHOKO HENMI,[1] FUMIHIKO SAKAMOTO,[1] AKIHIRO NARITA,[1] MASATO SHIMIZU,[1] KAZUHIDE TANIMURA,[1] MEGUMI MATSUHASHI,[1] TAMOTSU KAMISHIMA,[2] TATSUYA ATSUMI,[3] AND TAKAO KOIKE[3]

Objective. **To investigate the relationship between synovial vascularity assessed by quantitative power Doppler sonography (PDS) and progression of structural bone damage in a single finger joint in patients with rheumatoid arthritis (RA).**
Methods. **We studied 190 metacarpophalangeal (MCP) joints and 190 proximal interphalangeal (PIP) joints of 19 patients with active RA who had initial treatment with disease-modifying antirheumatic drugs (DMARDs). Patients were examined by clinical and laboratory assessments throughout the study. Hand and foot radiography was performed at baseline and the twentieth week. Magnetic resonance imaging (MRI) was performed at baseline. PDS was performed at baseline and the eighth week. Synovial vascularity was evaluated according to both quantitative and semiquantitative methods.**
Results. **Quantitative PDS was significantly correlated with the enhancement rate of MRI in each single finger joint. Comparing quantitative synovial vascularity and radiographic change in single MCP or PIP joints, the level of vascularity at baseline showed a significant positive correlation with radiographic progression at the twentieth week. The change of vascularity in response to DMARDs, defined as the percentage change in vascularity by the eighth week from baseline, was inversely correlated with radiographic progression in each MCP joint. The quantitative PDS method was more useful than the semiquantitative method for the evaluation of synovial vascularity in a single finger joint.**
Conclusion. **The change of synovial vascularity in a single finger joint determined by quantitative PDS could numerically predict its radiographic progression. Using vascularity as a guide to consider a therapeutic approach would have benefits for patients with active RA.**

INTRODUCTION

In recent years, the therapeutic goal for rheumatoid arthritis (RA) has moved far beyond the traditional factors of clinical remission, defined by the American College of Rheumatology (ACR) core data set or the European League Against Rheumatism (EULAR) Disease Activity Score in 28 joints (DAS28) remission criteria (1,2). To halt the progression of bone destruction, there has been a great need for a reliable predictive indicator of radiographic progression. Modern imaging techniques such as power Doppler sonography (PDS) and magnetic resonance imaging (MRI) have the potential to predict bone destruction (3–6). However, the relationship between therapeutic efficacy and image responses of these techniques has not been established.

PDS has several advantages in terms of medical cost and safety compared with other modern imaging techniques; therefore, it is more practical to use it repeatedly for monitoring disease activity. PDS detects the abnormal synovial vascular flow related to inflammation and has the potential to evaluate the level to represent this as a measurable

Clinical Trials Registration: UMIN 000002036.
[1]Jun Fukae, MD, PhD, Yujiro Kon, MD, PhD, Mihoko Henmi, MT, Fumihiko Sakamoto, MT, Akihiro Narita, MT, Masato Shimizu, MD, Kazuhide Tanimura, MD, Megumi Matsuhashi, MD: Tokeidai Memorial Hospital, Sapporo, Japan; [2]Tamotsu Kamishima, MD, PhD: Hokkaido University Hospital, Sapporo, Japan; [3]Tatsuya Atsumi, MD, PhD, Takao Koike, MD, PhD: Hokkaido University Graduate School of Medicine, Sapporo, Japan.
Address correspondence and reprint requests to Jun Fukae, MD, PhD, Center for Rheumatic Diseases, Tokeidai Memorial Hospital, Kita-1, Higashi-1, Cyuo-ku, Sapporo 060-0031, Japan. E-mail: jun.fukae@ryumachi-jp.com.
Submitted for publication October 8, 2009; accepted in revised form January 14, 2010.

Table 1. Clinical and laboratory characteristics of patients at baseline and the eighth and twentieth weeks*

	Baseline	8th week	20th week
Age, mean (range) years	54 (24–87)		
Sex, female/male	17/2		
RF positive, yes/no	15/4		
Prior use of DMARDs, yes/no	3/16		
Duration of symptoms, months	5 (3–11)		
Swollen joint count	3 (2–7)	1 (0–2)	0 (0–2)
Tender joint count	6 (2.5–13)	2 (1–5)	1 (1–1.5)
Patient's global assessment by VAS	60 (45–60)	29 (20.5–43.5)	25 (15.5–30)
ESR, mm/hour	43 (27–80)	24 (16–58)	27 (16–35)
CRP level, mg/dl	0.5 (0.25–2.82)	0.12 (0.1–1.1)	0.1 (0.1–1.4)
DAS28-ESR, mean ± SD mm/hour	5.21 ± 1.39	4.08 ± 1.60	3.56 ± 1.31

* Values are the median (interquartile range) unless otherwise indicated. RF = rheumatoid factor; DMARDs = disease-modifying antirheumatic drugs; VAS = visual analog scale; ESR = erythrocyte sedimentation rate; CRP = C-reactive protein; DAS28 = Disease Activity Score in 28 joints.

parameter (7,8). With growing interest in the ability to define remission in RA, it has been reported that abnormal synovial vascular flow still remains in individual joints after achievement of clinical remission, and therefore bone destruction would progress at a high rate in such cases (3,9). In this sense, direct assessment of synovial vascular flow in a single joint would be of use. Semiquantitative scoring has been widely used to evaluate synovial vascularity (10,11). The scoring was divided into 4 steps that were judged subjectively by the observer, and represented, accordingly, as a semiquantitative approach. The relationship between synovial vascular changes and progression of structural bone damage in a single joint has been the focus of much investigation, but only a few studies have been successful despite the intensive attempts of many researchers (3,12–14). In our preliminary study, we established quantitative PDS for synovial vascularity in each finger joint (15,16). The measurement was able to assess vascularity as quantitative data, objectively determined by the ultrasonographic program, and to detect small changes in individual finger joints. We investigated the relationship between synovial vascular changes and progression of structural bone damage in a single finger joint using the quantitative PDS measurement. We further defined the vascularity in response to disease-modifying antirheumatic drugs (DMARDs) by imaging and investigated its clinical significance in patients with active RA.

PATIENTS AND METHODS

Patients. Nineteen new patients with RA were enrolled in the study. All of the patients satisfied the ACR (formerly the American Rheumatism Association) 1987 diagnostic criteria (17). All of the patients were diagnosed as having the active state of RA according to the DAS28–erythrocyte sedimentation rate (ESR; >2.7 mm/hour). Demographic, clinical, and laboratory characteristics of the patients are shown in Table 1. Three patients were already receiving DMARDs at the initial diagnosis, but they were having no therapeutic effect (1 patient with sulfasalazine [SSZ], 2 patients with auranofin). After baseline examinations, all of the patients were given one of the new DMARDs. Initial treatments were continued throughout the study, but additional treatment and escalating doses of DMARDs were permitted in cases with disease exacerbation after the eighth week. We performed clinical and imaging examinations as mentioned in each section.

The study was conducted in accordance with the Helsinki Declaration. Informed consent to the protocol approved by the ethics committee of the hospital was obtained from all of the patients.

Ultrasonography and assessment. Ultrasonography was performed at baseline and the eighth week by 1 of the 3 ultrasonographers (MH, FS, AN) specialized in musculoskeletal ultrasonography who were blinded to other clinical information. A 13-MHz linear array transducer was used (HITACHI EUP-L34P). Pulse Doppler settings were standardized for the detection of synovial blood flow by adjusting color gain, pulse repetition, and flow optimization parameters according to a previous study (15). Power Doppler settings (75 dB dynamic range, medium persistence, medium frame rate, low wall filter, 1,300 Hz pulse repetition frequency, flow optimization: medium vein, 1,300 Hz speed velocity) were identical throughout the examinations. Room temperature was kept at 25°C. The patients were positioned comfortably, and the examinations were then started after 10 minutes of stabilization of the pulse rate. The scanning technique on each finger joint was standardized and fixed as follows: scanning of the first through fifth metacarpophalangeal (MCP) joints and the first through fifth proximal interphalangeal (PIP) joints was performed in the longitudinal plane over the dorsal surface of the joint with light skin pressure. The basic scanning technique followed the EULAR guidelines (18). The synovial vascular area with the most pronounced power Doppler activity was identified from the cine-loop and stored. The PDS images were recorded in the hard disk of the ultrasonographic machine. All of the examinations were completed within 15 minutes. Semiquantitative scoring has been described in previous studies (0 = absence of signal, 1 = single vessel dots, 2 = vessel dots over less than

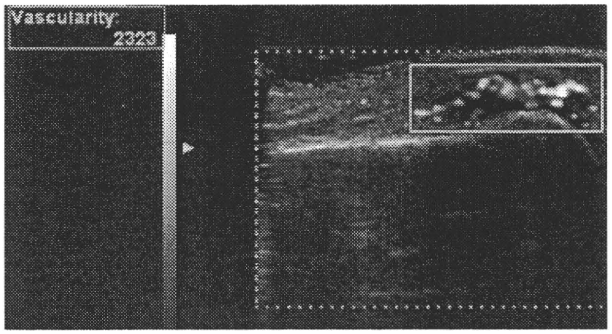

Figure 1. An image of finger joint ultrasonography (right 5th metacarpophalangeal joint). Each joint was scanned as described in the Patients and Methods section. The white line box indicates the region of interest (ROI) that was located at synovial vascular flow. Pixels of vascular flow inside the ROI were measured by the ultrasonographic program and displayed at the upper left corner of the monitor.

half of the synovium area, 3 = vessel dots over greater than half of the synovium area) (10,11,19). A synovial vascularity value, measured by quantitative PDS, was defined as P-vasc, which is the number of vascular flow pixels in the region of interest (ROI). The ROI was a standardized box type (5 mm × 10 mm) that was located to contain as many of the vascular flow pixels as possible. Vascular flow pixels in the ROI were measured automatically using the program's Vascularity mode in the ultrasonographic machine (HITACHI EUB-6500) (Figure 1).

Radiography and assessment. Plain radiographs of the hands, wrists, and feet were obtained at baseline and the twentieth week. Radiologic assessments were examined according to the Genant-modified Sharp score (GSS) by a rheumatologist (YK) who was blinded to other clinical information (20).

MRI and assessment. MRIs of both finger joints were taken at baseline using the 1.5T system (Signa Excite, version 12) with a cardiac coil. During the examination, patients were placed in the supine position with both hands on the abdomen, and these were covered by the anterior segment of the cardiac coil. Dynamic 3-dimensional forkhead activin signal transducer spoiled gradient-recalled acquisition in the steady state T1-weighted coronal images (time to recovery 500 msec, time to echo 11 msec, field of view 30 cm, matrix 256 × 160, 20 slices, slice thickness 3 mm, gap 0.4 mm, imaging time 10, 17 loops with an interval time of 5 seconds) were obtained for both hands in addition to the other images with different scan sequences. A bolus injection of gadopentate dimeglumine (Gd-DTPA; 0.1 mmole/kg body weight) was administered at 1 ml/second via a 21-gauge indwelling needle inserted into an antecubital fossa vein during acquisition of the baseline images (first loop) of the dynamic study. Data were transferred from the MRI console to a Digital Imaging and Communication in Medicine viewer and then a workstation (Advantage Windows workstation) for quantitative analysis. The severity of synovitis has been previously assessed by the rate of enhancement (E-rate) in a dynamic study by injection of Gd-DTPA (21). The E-rate indicates the index of enhancement by plotting the signal intensity against time in a selected ROI (~20–30 mm^2 in area) of the site of maximum enhancement in the above-mentioned 20 joints. Image analysis was carried out by an experienced radiologist (TK) who was blinded to other clinical information.

Statistical analysis. Statistical analyses were calculated with the use of the Excel program and the MedCalc program, version 10.4.5.0. Differences between the 2 groups were examined using either Student's *t*-test or a nonparametric test (Wilcoxon's signed rank test, Mann-Whitney U test), as applicable. A correlation between 2 variables was examined using either a parametric test (Pearson's correlation test) or a nonparametric test (Spearman's rank correlation test) according to the distribution of values. Intra-and interobserver reliability of the semiquantitative PDS score was estimated using calculations of weighted kappa statistics and overall agreement. Intra-and interobserver reliability of P-vasc was estimated using calculations of intraclass correlation coefficients (ICCs). The smallest detectable change for the radiographic score change was calculated according to a previous study (22).

RESULTS

Clinical disease activity. The mean ± SD DAS28-ESR at baseline was 5.21 ± 1.39 mm/hour. The mean ± SD DAS28-ESR at the eighth week was 4.08 ± 1.60 mm/hour, which was significantly decreased from baseline (P = 0.0001). There was no significant difference in the DAS28-ESR between the eighth week and the twentieth week (P = 0.0741). At the twentieth week, 13 patients were receiving monotherapy (9 with methotrexate [MTX], 2 with SSZ, and 2 with bucillamine) and 6 patients were receiving combination therapy of DMARDs (3 with MTX plus bucillamine, 1 with MTX plus SSZ, 1 with SSZ plus bucillamine, and 1 with SSZ plus tacrolimus). Thirteen patients were receiving oral prednisolone (3–10 mg/day) at the twentieth week.

Intra-and interobserver reliability for PDS. All PDS images for MCP joints and PIP joints were blindly evaluated twice according to the semiquantitative score for each joint by 2 ultrasonographers (MH, AN). The obtained intraobserver kappa values of the semiquantitative score were 0.944 for MCP joints and 0.930 for PIP joints. The intraobserver overall agreement for these joints was 96% and 95.4%, respectively. The obtained interobserver kappa values of the semiquantitative score were 0.950 for MCP joints and 0.923 for PIP joints. The interobserver overall agreement for these joints was 95.7% and 97.1%, respectively.

Representative images for 20 MCP joints and 20 PIP joints were randomly chosen, and P-vasc was measured 3 times each by 3 ultrasonographers (MH, FS, AN). The obtained intraobserver ICC values were 0.990 for MCP joints and 0.990 for PIP joints. The interobserver ICC values were 0.990 for MCP joints and 0.990 for PIP joints.

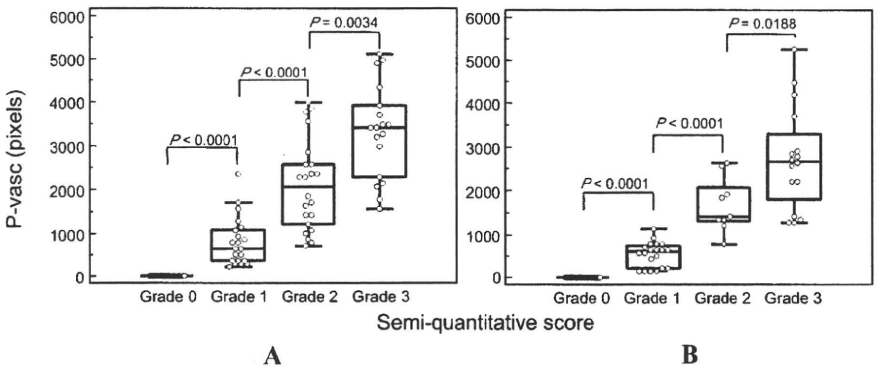

Figure 2. Relation between quantitative measurement and semi-quantitative scoring for synovial vascularity. The levels of synovial vascularity value (P-vasc) were plotted against semi-quantitative scores in MCP joints (**A**) and PIP joints (**B**).

Relationship of quantitative PDS measurement (P-vasc) to semiquantitative scoring for synovial vascularity and to the E-rate of MRI. The PDS images for 190 MCP joints and 190 PIP joints at baseline were evaluated using both the semiquantitative score and the P-vasc. The P-vasc significantly increased as the semiquantitative score increased in both MCP joints and PIP joints (Figure 2).

One patient was unable to undergo MRI because of claustrophobia. One hundred eighty MCP joints and 180 PIP joints of 18 patients were evaluated using both the P-vasc and E-rate. The P-vasc had a significant positive correlation with the E-rate of MRI in both MCP and PIP joints (Pearson's r = 0.739, $P < 0.0001$ and Pearson's r = 0.537, $P < 0.0001$, respectively) (Figure 3).

Association between vascularity and radiographic progression in a single joint. The median local GSS at baseline for MCP and PIP joints were 0 (interquartile range [IQR] 0–1) and 0.5 (IQR 0–1.5), respectively. The median local GSS at the twentieth week for MCP and PIP joints were 0.5 (IQR 0–1.5) and 0.75 (IQR 0–1.5), respectively. The median total GSS was 16.5 (IQR 11.3–37.3) at baseline. The median total GSS at the twentieth week was 30.0, which was significantly higher than the baseline score ($P = 0.001$).

We next focused on changes of single-joint P-vasc and local GSS. We investigated the association between the level of vascularity at baseline and radiographic progression at the twentieth week in each single finger joint. One hundred ninety MCP joints and 190 PIP joints at baseline were evaluated. The level of P-vasc at baseline significantly correlated with progression of the local GSS in both MCP and PIP joints (Spearman's $\rho = 0.466$, $P < 0.0001$ and Spearman's $\rho = 0.362$, $P < 0.0001$, respectively) (Figures 4A and B). The association between the semiquantitative score and the progression of the local GSS had the same tendency (data not shown). We took note of the positive PDS joints at baseline and calculated their improvement rate (IR), defined as the percentage change in P-vasc by the eighth week from baseline. The IR was calculated as follows: (P-vasc value at baseline − P-vasc value at eighth week)/P-vasc value at baseline × 100 (%). At baseline, 61 MCP joints and 44 PIP joints had positive PDS signals. The IR of P-vasc had a significant inverse correlation with local GSS progression in each single MCP joint (Spearman's $\rho = -0.340$, $P = 0.00386$) (Figure 5A). There was no significant correlation between the IR of P-vasc and local GSS progression in each single PIP joint (Spearman's $\rho = -0.223$, $P = 0.1430$) (Figure 5B). In the case of assessment by semiquantitative score, there was no significant correla-

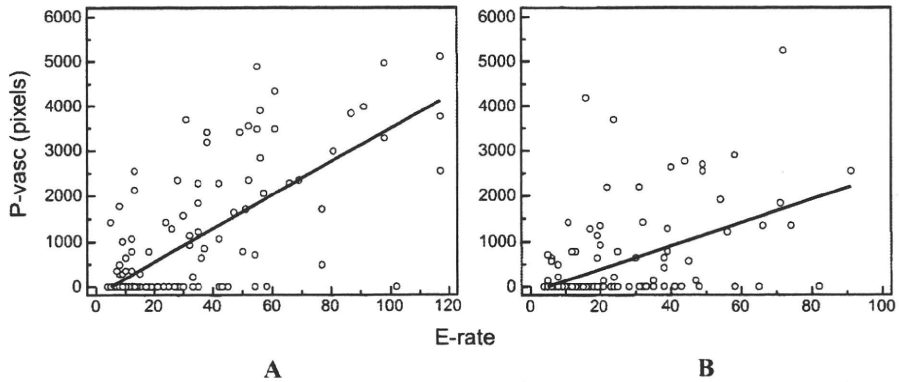

Figure 3. Relationship between quantitative measurement of synovial vascularity with power Doppler sonography and the index of synovial enhancement of magnetic resonance imaging (MRI). Scatter diagrams and regression lines of synovial vascularity value (P-vasc) against the enhancement rate (E-rate) of MRI in metacarpophalangeal joints (**A**) or proximal interphalangeal joints (**B**) are shown.

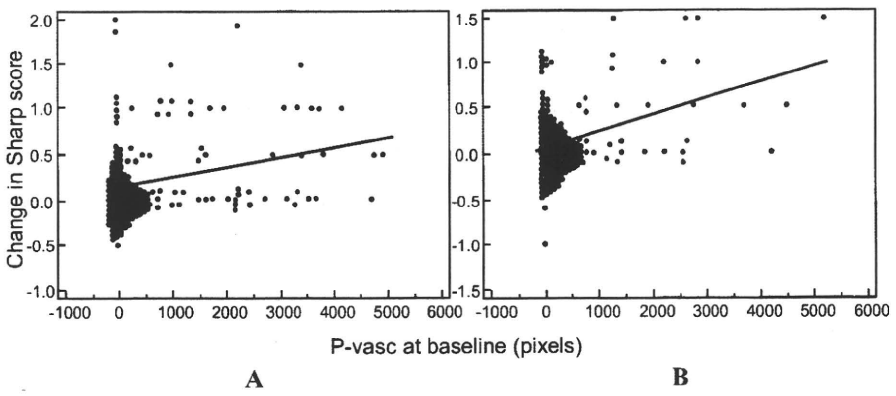

Figure 4. Relationship between the level of synovial vascularity and radiographic progression in each single finger joint. Scatter diagrams and regression lines of the synovial vascularity value (P-vasc) at baseline against progression of the local Genant-modified Sharp score from baseline to the twentieth week in metacarpophalangeal joints (**A**) or proximal interphalangeal joints (**B**) are shown.

tion to MCP or PIP joints (Spearman's $\rho = -0.256$, $P = 0.0579$ and Spearman's $\rho = -0.105$, $P = 0.5179$, respectively) (data not shown). The smallest detectable change values were calculated for the radiographic erosion score, joint space narrowing score, and combined score for single MCP and PIP joints (0.21–0.48). All of the calculated smallest detectable changes did not exceed the smallest unit of the scoring (0.5).

DISCUSSION

In this study, we quantitatively evaluated synovial vascularity in a single finger joint. In each finger joint, we found that a level of vascularity at baseline correlated with the radiographic progression. We also demonstrated that the change of vascularity in response to DMARD therapy could numerically predict the radiographic progression in each single finger joint.

We defined a standardized box type ROI and quantitatively evaluated synovial vascularity, as mentioned in the Patients and Methods section. All of the kappa values and ICCs calculated for intra-and interobserver reliability during the PDS measurements were acceptable in this study.

To demonstrate the validity of our quantitative PDS method, we first examined a relationship between the P-vasc and semiquantitative scoring. The P-vasc significantly increased in parallel with semiquantitative scoring. The E-rate of MRI is an index of Gd-DTPA enhancement indicating the inflammatory level (21,23,24), and was used for comparing with quantitative ^{99m}Tc-labeled nanocolloid scintigraphy for assessing RA (25). We next examined the relationship between the E-rate and P-vasc. Although the P-vasc was not detected in some joints with a high E-rate, a positive significant correlation was shown between the E-rate and P-vasc, suggesting that synovial vascularity determined by our quantitative PDS reflects, in part, the inflammatory level. The main reason of discrepancy between a joint with a high E-rate and negative PDS should be explained by the fact that MRI covered inflammation from all sites of synovial tissue, whereas PDS detected only from the dorsal side of synovial tissue. In addition, the difference of sensitivity of PDS and that of the E-rate might be a problem. Because the PDS is one of the advancing modalities for imaging rheumatic joints, there would be many more points to be improved in the

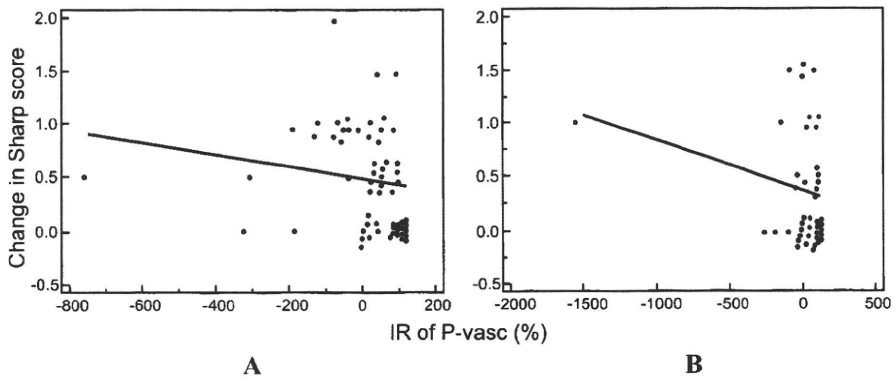

Figure 5. Relationship between improvement of synovial vascularity and radiographic progression in each single finger joint. Scatter diagrams and regression lines of the improvement rate (IR) for synovial vascularity value (P-vasc) between baseline and the eighth week against progression of the local Genant-modified Sharp score from baseline to the twentieth week in metacarpophalangeal joints (**A**) or proximal interphalangeal joints (**B**) are shown.

technological aspects, and such a process will promise to overcome the current problems in the future.

We used the P-vasc for investigating the relationship between the change of synovial vascularity and radiographic progression in a single finger joint. We found that, for each single finger joint, the baseline P-vasc significantly correlated with progression of the local GSS over 20 weeks. Our study, for the first time, has quantitatively confirmed the recent reports of Brown et al and Naredo et al that the presence of vascularity using PDS in a qualitative way correlated with the bone destruction in each single joint (3,13).

We next focused on PDS-positive finger joints at baseline and calculated each IR from baseline to the eighth week. The IR of P-vasc had a significant inverse correlation with radiographic progression in each single MCP joint. It was a novel finding that improvement in the rate of vascularity resulted in the suppression of radiographic progression. The semiquantitative score failed to demonstrate the same tendency due to its low sensitivity at detecting small changes in vascularity. On the other hand, the IR of P-vasc in PIP joints was not significantly correlated with radiographic progression, presumably due to either the sample size or the ROI setting. Further refinement of ROIs specific to PIP joints may improve the accuracy of the technique.

According to the 2002 ACR guidelines for the treatment of RA, therapeutic evaluation of first-line DMARDs was assessed at 8–12 weeks using clinical indices (26). Naredo et al reported that the time-integrated value of the PDS parameters correlated with the radiographic progression over 1 year (13), suggesting that rapid reduction in the PDS signal could predict a better radiologic prognosis. The IR of P-vasc, a change rate of 2 points, could be a useful index for preventing bone destruction. A quantitative PDS method was more useful than a semiquantitative method to detect change of synovial vascularity in each single finger joint.

Although this is a preliminary study with a small number of patients, it is noteworthy that the clinical implications of our results include the potential of synovial vascularity to numerically predict an outcome of bone destruction in each single finger joint. Furthermore, we found that the change of vascularity influenced radiographic progression. The IR of synovial vascularity should be an index of therapeutic efficacy, and therefore be of value in making judgments about additional treatment with DMARDs or to change to early biologic agent therapy. Using vascularity as guide to make therapeutic decisions at early stages would have benefits for patients with active RA. Larger and longitudinal studies would indicate the efficacy of PDS for the better management of affected patients.

ACKNOWLEDGMENT

We thank the secretary in our hospital, Ms Akemi Kitano, for data collection.

AUTHOR CONTRIBUTIONS

All authors were involved in drafting the article or revising it critically for important intellectual content, and all authors approved the final version to be submitted for publication. Dr. Fukae had full access to all of the data in the study and takes responsibility for the integrity of the data and the accuracy of the data analysis.

Study conception and design. Fukae, Kon, Tanimura, Kamishima, Atsumi, Koike.

Acquisition of data. Fukae, Kon, Henmi, Sakamoto, Narita, Shimizu, Tanimura, Matsuhashi, Kamishima.

Analysis and interpretation of data. Fukae, Kon, Henmi, Sakamoto, Narita, Shimizu, Tanimura, Matsuhashi, Kamishima, Atsumi, Koike.

REFERENCES

1. Felson DT, Anderson JJ, Boers M, Bombardier C, Furst D, Goldsmith C, et al. American College of Rheumatology preliminary definition of improvement in rheumatoid arthritis. Arthritis Rheum 1995;38:727–35.
2. Prevoo ML, van 't Hof MA, Kuper HH, van Leeuwen MA, van de Putte LB, van Riel PL. Modified disease activity scores that include twenty-eight–joint counts: development and validation in a prospective longitudinal study of patients with rheumatoid arthritis. Arthritis Rheum 1995;38:44–8.
3. Brown AK, Conaghan PG, Karim Z, Quinn MA, Ikeda K, Peterfy CG, et al. An explanation for the apparent dissociation between clinical remission and continued structural deterioration in rheumatoid arthritis. Arthritis Rheum 2008;58:2958–67.
4. Freeston JE, Brown AK, Hensor EM, Emery P, Conaghan PG. Extremity magnetic resonance imaging assessment of synovitis (without contrast) in rheumatoid arthritis may be less accurate than power Doppler ultrasound [letter]. Ann Rheum Dis 2008;67:1351.
5. Freeston JE, Bird P, Conaghan PG. The role of MRI in rheumatoid arthritis: research and clinical issues. Curr Opin Rheumatol 2009;21:95–101.
6. Haavardsholm EA, Ostergaard M, Hammer HB, Boyesen P, Boonen A, van der Heijde D, et al. Monitoring anti-TNFα treatment in rheumatoid arthritis: responsiveness of magnetic resonance imaging and ultrasonography of the dominant wrist compared to conventional measures of disease activity and structural damage. Ann Rheum Dis 2009;68:1572–9.
7. Naredo E, Bonilla G, Gamero F, Uson J, Carmona L, Laffon A. Assessment of inflammatory activity in rheumatoid arthritis: a comparative study of clinical evaluation with grey scale and power Doppler ultrasonography. Ann Rheum Dis 2005;64:375–81.
8. Szkudlarek M, Narvestad E, Klarlund M, Court-Payen M, Thomsen HS, Ostergaard M. Ultrasonography of the metatarsophalangeal joints in rheumatoid arthritis: comparison with magnetic resonance imaging, conventional radiography, and clinical examination. Arthritis Rheum 2004;50:2103–12.
9. Brown AK, Quinn MA, Karim Z, Conaghan PG, Peterfy CG, Hensor E, et al. Presence of significant synovitis in rheumatoid arthritis patients with disease-modifying antirheumatic drug–induced clinical remission: evidence from an imaging study may explain structural progression. Arthritis Rheum 2006;54:3761–73.
10. Newman JS, Laing TJ, McCarthy CJ, Adler RS. Power Doppler sonography of synovitis: assessment of therapeutic response. Preliminary observations. Radiology 1996;198:582–4.
11. Hau M, Schultz H, Tony HP, Keberle M, Jahns R, Haerten R, et al. Evaluation of pannus and vascularization of the metacarpophalangeal and proximal interphalangeal joints in rheumatoid arthritis by high-resolution ultrasound (multidimensional linear array). Arthritis Rheum 1999;42:2303–8.
12. Taylor PC, Steuer A, Gruber J, Cosgrove DO, Blomley MJ, Marsters PA, et al. Comparison of ultrasonographic assessment of synovitis and joint vascularity with radiographic

evaluation in a randomized, placebo-controlled study of infliximab therapy in early rheumatoid arthritis. Arthritis Rheum 2004;50:1107–16.
13. Naredo E, Collado P, Cruz A, Palop MJ, Cabero F, Richi P, et al. Longitudinal power Doppler ultrasonographic assessment of joint inflammatory activity in early rheumatoid arthritis: predictive value in disease activity and radiologic progression. Arthritis Rheum 2007;57:116–24.
14. Taylor PC, Steuer A, Gruber J, McClinton C, Cosgrove DO, Blomley MJ, et al. Ultrasonographic and radiographic results from a two-year controlled trial of immediate or one-year–delayed addition of infliximab to ongoing methotrexate therapy in patients with erosive early rheumatoid arthritis. Arthritis Rheum 2006;54:47–53.
15. Kamishima T, Tanimura K, Henmi M, Narita A, Sakamoto F, Terae S, et al. Power Doppler ultrasound of rheumatoid synovitis: quantification of vascular signal and analysis of interobserver variability. Skeletal Radiol 2009;38:467–72.
16. Fukae J, Shimizu M, Kon Y, Tanimura K, Matsuhashi M, Kamishima T, et al. Screening for rheumatoid arthritis with finger joint power Doppler ultrasonography: quantification of conventional power Doppler ultrasonographic scoring. Mod Rheumatol 2009;19:502–6.
17. Arnett FC, Edworthy SM, Bloch DA, McShane DJ, Fries JF, Cooper NS, et al. The American Rheumatism Association 1987 revised criteria for the classification of rheumatoid arthritis. Arthritis Rheum 1988;31:315–24.
18. Backhaus M, Burmester GR, Gerber T, Grassi W, Machold KP, Swen WA, et al. Guidelines for musculoskeletal ultrasound in rheumatology. Ann Rheum Dis 2001;60:641–9.
19. Meenagh G, Filippucci E, Delle Sedie A, Riente L, Iagnocco A, Epis O, et al. Ultrasound imaging for the rheumatologist. XVIII. Ultrasound measurements. Clin Exp Rheumatol 2008; 26:982–5.
20. Genant HK, Jiang Y, Peterfy C, Lu Y, Redei J, Countryman PJ. Assessment of rheumatoid arthritis using a modified scoring method on digitized and original radiographs. Arthritis Rheum 1998;41:1583–90.
21. Ostergaard M, Stoltenberg M, Lovgreen-Nielsen P, Volck B, Sonne-Holm S, Lorenzen I. Quantification of synovitis by MRI: correlation between dynamic and static gadolinium-enhanced magnetic resonance imaging and microscopic and macroscopic signs of synovial inflammation. Magn Reson Imaging 1998;16:743–54.
22. Bruynesteyn K, Boers M, Kostense P, van der Linden S, van der Heijde D. Deciding on progression of joint damage in paired films of individual patients: smallest detectable difference or change. Ann Rheum Dis 2005;64:179–82.
23. Tamai M, Kawakami A, Uetani M, Takao S, Tanaka F, Fujikawa K, et al. Bone edema determined by magnetic resonance imaging reflects severe disease status in patients with early-stage rheumatoid arthritis. J Rheumatol 2007;34: 2154–7.
24. Szkudlarek M, Court-Payen M, Strandberg C, Klarlund M, Klausen T, Ostergaard M. Power Doppler ultrasonography for assessment of synovitis in the metacarpophalangeal joints of patients with rheumatoid arthritis: a comparison with dynamic magnetic resonance imaging. Arthritis Rheum 2001;44: 2018–23.
25. Palosaari K, Vuotila J, Takalo R, Jartti A, Niemela R, Haapea M, et al. Contrast-enhanced dynamic and static MRI correlates with quantitative 99Tcm-labelled nanocolloid scintigraphy: study of early rheumatoid arthritis patients. Rheumatology (Oxford) 2004;43:1364–73.
26. American College of Rheumatology Subcommittee on Rheumatoid Arthritis Guidelines. Guidelines for the management of rheumatoid arthritis: 2002 update. Arthritis Rheum 2002; 46:328–46.

Increased Expression of Phospholipid Scramblase 1 in Monocytes from Patients with Systemic Lupus Erythematosus

ERIKO SUZUKI, OLGA AMENGUAL, TATSUYA ATSUMI, KENJI OKU, TOKO HASHIMOTO, HIROSHI KATAOKA, TETSUYA HORITA, SHINSUKE YASUDA, MASAHIRO IEKO, KAZUAKI FUKUSHIMA, and TAKAO KOIKE

ABSTRACT. ***Objective.*** A high incidence of thromboembolic events has been reported in patients with systemic lupus erythematosus (SLE). Phosphatidylserine (PS) is normally sequestered in the inner leaflet of cell membranes. Externalization of PS during cell activation is mediated by phospholipid scramblase 1 (PLSCR1) and has a central role in promoting blood coagulation. We investigated the underlying pathogenic status of thrombophilia in SLE by analyzing PLSCR1 expression on monocytes from patients with SLE.

Methods. Sixty patients with SLE were evaluated. Twenty-three patients had antiphospholipid syndrome (APS/SLE). Plasma D-dimer levels were measured as a marker of fibrin turnover. The cDNA encoding human PLSCR1 was cloned from the total RNA extract from monocytes, and independent clones were sequenced. PLSCR1 mRNA expression in CD14+ cells was determined by real-time polymerase chain reaction. PS exposure on CD14+ cell surface was analyzed by flow cytometry.

Results. Elevated D-dimer levels were found in plasma from SLE patients. Three splice variants of PLSCR1 mRNA were identified in all subjects, and levels of full-length PLSCR1 mRNA were significantly increased in SLE compared to healthy controls (2.9 ± 1.5 vs 1.3 ± 0.4, respectively; $p < 0.0001$). Flow-cytometry analysis showed relative enhancement of PS exposure in the surface of CD14+ cells in SLE patients compared to healthy controls.

Conclusion. Novel PLSCR1 splice variants were identified. Monocytes in SLE patients had enhanced PLSCR1 mRNA expression, as well as increased fibrin turnover and cell-surface PS exposure, indicating that PLSCR1 may, in part, contribute to the prothrombotic tendency in SLE. (First Release June 1 2010; J Rheumatol 2010;37:1639–45; doi:10.3899/jrheum.091420)

Key Indexing Terms:
THROMBOSIS
ANTIPHOSPHOLIPID SYNDROME
AUTOIMMUNE DISEASES
SYSTEMIC LUPUS ERYTHEMATOSUS

Systemic lupus erythematosus (SLE) is an autoimmune disease characterized by acute/chronic inflammation linked with the production of autoantibodies, generation of circulating immune complexes, and activation of the complement system. Thrombotic events are frequent manifestations observed in more than 10% of patients with SLE[1,2]. The etiology of thrombosis is multifactorial and might be related to premature atherosclerosis, vasculitis, and hypercoagulability. Several environmental or genetic risk factors have been reported to increase this tendency, but the precise thrombotic mechanisms in SLE are not yet clarified[3].

Hypercoagulability in SLE is typically due to the presence of antiphophospholipid antibodies (aPL), complicated with the antiphospholipid syndrome (APS)[4]. aPL belong to a large family of autoantibodies directed against phospholipid-binding plasma proteins or against the complex of these proteins with anionic phospholipids[5].

Phosphatidylserine (PS) is an anionic phospholipid normally sequestered in the inner leaflet of the cell membrane. Externalization of PS occurs in activated cells and plays a

From the Department of Medicine II, Hokkaido University Graduate School of Medicine; Department of Dental Anesthesiology, Hokkaido University Graduate School of Dental Medicine, Sapporo, Japan; and Department of Internal Medicine, School of Dentistry, Health Sciences University of Hokkaido, Ishikari-Tobetsu, Hokkaido, Japan.

Supported by the Japanese Ministry of Health, Labour, and Welfare; the Japanese Ministry of Education, Culture, Sports, Science and Technology (MEXT); and the Japanese Society for the Promotion of Science (JSPS). Dr. Amengual is a postdoctoral researcher supported by JSPS/MEXT (grant 0940106, Project number 21-40106).

E. Suzuki, DDS, Department of Medicine II, Hokkaido University Graduate School of Medicine, Department of Dental Anesthesiology, Hokkaido University Graduate School of Dental Medicine; O. Amengual, MD, PhD; T. Atsumi, MD, PhD; K. Oku, MD, PhD; T. Hashimoto, MD, PhD; H. Kataoka, MD, PhD; T. Horita, MD, PhD; S. Yasuda, MD, PhD, Department of Medicine II, Hokkaido University Graduate School of Medicine; M. Ieko, MD, PhD, Department of Internal Medicine, School of Dentistry, Health Sciences University of Hokkaido; K. Fukushima, DDS, PhD, Department of Dental Anesthesiology, Hokkaido University Graduate School of Dental Medicine; T. Koike, MD, PhD, Department of Medicine II, Hokkaido University Graduate School of Medicine.

Address correspondence to Dr. T. Atsumi, Department of Medicine II, Hokkaido University Graduate School of Medicine, N15 W7, Kita-ku, Sapporo 060-8638, Japan. E-mail: at3tat@med.hokudai.ac.jp

Accepted for publication March 23, 2010.

central role in promoting blood coagulation, as PS serves as a catalytic surface for the assembly of the coagulation factors, including the prothrombinase and tenase complex[6]. The exposure of PS at the outer leaflet of the plasma membrane is also essential for the binding of aPL to procoagulant cells. Several groups have reported the crucial role of the p38 mitogen-activated protein kinase (MAPK) pathway in aPL-mediated cell activation[7,8]. In order that aPL bind and activate cells, the immune complexes have to be present on the PS-exposed cell surface[9]. One of the key molecules involved in regulation of PS externalization during cell activation is phospholipid scramblase 1 (PLSCR1), which catalyzes rapid transbilayer movement of phospholipids between membrane leaflets. PLSCR1 is a lipid-raft associated type II plasma protein of about 37 kDa containing 318 amino acid residues with a long N-terminal cytoplasmic domain, a transmembrane helix region, and a short extracellular tail[10].

Although plasma membrane asymmetry is the rule for normal cells, loss of asymmetry, especially the appearance of PS at the cell surface, is associated with physiological and pathological phenomena, including thrombosis[11]. In order to investigate the underlying pathogenic status of thrombophilia in SLE, we examined the expression of PLSCR1 on procoagulant cells from patients with SLE.

MATERIALS AND METHODS

Patients. Sixty unselected consecutive Japanese patients with SLE who visited the Rheumatic and Connective Tissue Disease Clinic were recruited. All patients, 57 women and 3 men, mean age 45 years (range 23–70 yrs), fulfilled the American College of Rheumatology criteria for SLE[12]. Twenty-three patients (38%) were diagnosed as having APS in association with SLE. APS was diagnosed according to the revised international criteria for APS[13].

The mean SLE disease duration was 15.5 ± 9.9 years (range 0.5–42 yrs). No patient had thrombosis or pregnancy complications within 3 months before blood collection. Signs of acute thrombosis were not detected in any patient at the time blood was drawn. Lupus activity was assessed by certified rheumatologists at the time of blood sampling by analyzing laboratory data such as white blood cells and platelet count, hemoglobin levels, C-reactive protein (CRP), C3, C4 and CH50 levels, anti-DNA antibodies, and clinical manifestations. The historical profile of clinical and laboratory manifestations and SLE Disease Activity Index (SLEDAI)[14] were verified by the authors using medical records, as summarized in Table 1.

When blood was drawn, 8 patients were receiving warfarin (13%). No patients were taking heparin.

Blood samples were also collected from 43 apparently healthy Japanese individuals who consented to join the study (25 women and 18 men, mean age 28 yrs, range 20–38 yrs).

The study was performed in accordance with the Declaration of Helsinki and the Principles of Good Clinical Practice. Approval was obtained from the local ethics committee, and informed consent was obtained from each subject before enrollment.

Plasma samples. Venous blood was collected into tubes containing sodium citrate and was centrifuged immediately at 4°C. Plasma samples were depleted of platelets by filtration then stored at –80°C.

Plasma D-dimer determination. Plasma D-dimer levels (Nanopia, D-dimer, Daiichi Kagaku, Tokyo, Japan) were measured as markers of fibrin turnover. The cutoff level was previously defined as > 95th percentile of 65 healthy subjects (34 women. 31 men, mean age 40 yrs, range 18–76), as a routine laboratory assay.

Table 1. Profile of patients.

Characteristic		
Diagnosis, no. (%)		
Non-APS	37	(62)
APS	23	(38)
Age, yrs, mean (range)	45	(23–70)
Female:male	57:3	
Historical manifestations, no. (%)		
Photosensitivity	26	(43)
Oral ulcers	16	(27)
Skin	37	(62)
Arthritis	42	(70)
Serositis	14	(23)
Nephritis	30	(50)
Central nervous system	18	(30)
Hematological	50	(83)
Thrombosis	23	(38)
Arterial	14	(23)
Venous	12	(20)
Arterial and venous	2	(3)
Pregnancy morbidity	6	(11)
At the time of blood testing*		
SLEDAI, mean (range)	2.5	(0–10)
aPL		
aCL IgG/M	8/2	(13)/(3)
Anti-$ß_2$-GPI IgG/M	11/3	(18)/(5)
LAC	20	(33)
Other laboratory data, mean ± SD (range)		
White blood cells, × $10^3/\mu l$	6.8 ± 2.7	(2.1–14.1)
Platelets, × $10^3/\mu l$	230 ± 75	(88–433)
Hemoglobin, g/l	12.5 ± 1.7	(8.2–16.9)
CRP, mg/dl*	0.09	(0.02–3)
C3, mg/dl	85.3 ± 22.1	(46–148)
C4, mg/dl	18.6 ± 8.1	(4–41)
CH50, U/ml	45.3 ± 12.2	(17.3–72)
Anti-DNA antibodies, IU/ml*	5	(0–59)

* Median (range). SLE: systemic lupus erythematosus, APS: antiphospholipid syndrome, aPL: antiphospholipid antibodies, aCL: anticardiolipin antibodies, anti-$ß_2$-GPI: anti-$ß_2$-glycoprotein I antibodies, CRP: C-reactive protein, IU: international units.

Antiphospholipid antibody determination. IgG and IgM anticardiolipin antibodies (aCL) were assayed according to the standard aCL enzyme-linked immunosorbent assay (ELISA)[15]. IgG and IgM anti-$ß_2$-glycoprotein I (anti-$ß_2$-GPI) antibodies were determined by in-house ELISA as described[16]. Normal ranges of IgG (< 18 GPL) and IgM (< 30 MPL) aCL, and IgG (< 2.2 U/ml) and IgM (< 6.0 U/ml) anti-$ß_2$-GPI antibodies, were established using 132 healthy controls with 99th percentile cutoff values.

For the detection of lupus anticoagulant (LAC) guidelines recommended by the Subcommittee on Lupus Anticoagulant/Antiphospholipid Antibody of the Scientific and Standardisation Committee of the International Society of Thrombosis and Haemostasis were followed[17].

Isolation and preparation of cells. Venous blood was collected into tubes containing heparin and processed at room temperature (RT) within 3 hours. Peripheral blood mononuclear cells (PBMC) were isolated on Ficoll-Paque plus® gradient centrifugation (Amersham Biosciences, Uppsala, Sweden) using standard protocols. PBMC were pelleted by centrifugation, and washed twice with phosphate buffered saline (PBS; Sigma, St Louis, MO, USA). Contaminated red blood cells were then lysated with red blood cell

lysis buffer (eBioscience, San Diego, CA, USA) at RT for 10 min and washed twice with PBS. Monocytes were purified using CD14 microbeads (Miltenyi Biotec, Bergisch Gladbach, Germany) as follows: PBMC pellet was suspended in 80 μl of auto MACS™ rinsing solution (Miltenyi Biotec), and 20 μl of CD14 microbeads were added. After 15 min incubation at 4°C, cells were washed with 2 ml of MACS rinsing solution, suspended in 500 μl of MACS rinsing solution, and separated in a magnetic separation kit (Miltenyi Biotec) according to manufacturer's instructions.

RNA extraction and reverse transcription-polymerase chain reaction (RT-PCR). Total RNA were isolated from PBMC or monocytes using RNeasy Mini Kit (Qiagen, Valencia, CA, USA) and reverse-transcribed with the SuperScript™ First-Strand Synthesis System for RT-PCR (Invitrogen, Carlsbad, CA, USA). cDNA were amplified using a pair of primers corresponding to sequences residing at the beginning and the end of the coding domain of the normal human PLSCR1 transcript noted at GenBank accession NM_021105. The gene-specific primer sequences were as follows: forward 5'-GCT CTC TGG ACC TTG TCT CG-3' and reverse primer 5'-CCA GAG CTA CAG GCC TTA CAG-3'. PCR was performed in 31 cycles of 95°C for 30 s, 61°C for 30 s, and 72°C for 45 s, followed by a final extension step 72°C for 7 min. The amplified products were resolved in 9% polyacrylamide gels, stained with ethidium bromide, and visualized under ultraviolet light. The housekeeping gene glyceraldehyde-3-phosphate dehydrogenase (GAPDH) was used as control using the following gene-specific primer sequences: forward 5'-ACA TCG CTC AGA CAC CAT GG-3' and reverse 5'-GTA GTT GAG GTC AAT GAA GGG-3'. RT-PCR for GAPDH was performed in 28 cycles of 95°C for 45 s, 54°C for 45 s, and 72°C for 45 s, followed by a final extension step at 72°C for 7 min. Bands of 150 bp were identified for GAPDH in 9% polyacrylamide gels.

Cloning and sequencing of PLSCR1 cDNA. Amplification of PLSCR1 was done using the PCR method described above. PCR products were separated by electrophoresis in 1% agarose gels and visualized with ethidium bromide. Four fragments of 1122 bp, 905 bp, 750 bp, and 551 bp were identified, separately recovered from the gel using MiniElute Gel Extraction Kit (Qiagen), and subsequently cloned into a pcDNA3.1 V5-His©-TOPO® TA expression kit (Invitrogen). Transformed *Escherichia coli* clones were randomly selected and screened with the QIAprep Spin Miniprep kit (Qiagen) and BstX1 restriction enzyme (New England BioLabs, Beverly, MA, USA). Nucleotide sequences of independent clones from samples of 2 healthy donors were determined using a Centri Spin^{-20} column (Princeton Separations, Adelphi, NJ, USA), and ABI Prism 3130 Genetic Analyzer (Applied Biosystems, ABI, Foster City, CA, USA). Sequence alignments were analyzed by the AlignIR version 1.2 (LI-COR) software system, and homology search was carried out using BLAST programs.

Quantitative real-time PCR. Quantitative analysis of gene expression was performed by real-time PCR using ABI Prism 7700® Sequence Detection System (Applied Biosystems) and gene-specific TaqMan MGB probe for PLSCR1 (Hs01062169_m1) (Applied Biosystems), which recognize the junction sequence between exon 3 and 4 of human PLSCR1. The level of the PLSCR1 transcript was normalized to that of the GAPDH using TaqMan MGB GAPDH probe (Hs99999905_m1). Relative quantification was done using the comparable cycle threshold method as described[18].

Western blot analysis. For Western blot analysis of PLSCR1 protein, PBMC from a healthy donor were incubated in the presence or absence of interferon-α2a (IFN, 400 IU/ml; Santa Cruz Chemical Co., Santa Cruz, CA, USA) for 24 h in a 5% CO_2 atmosphere at 37°C. Cells were kept in RPMI-1640 medium (Sigma) supplemented with 10% fetal calf serum (Gibco BRL, Paisley, UK) containing penicillin and streptomycin. After incubation, PBMC were lysed in 30 μl × 10^6 cells of lysis buffer (2% NP-40 in PBS containing 5 mM EDTA, 50 mM benzamidine, 50 mM N-ethylmaleimide, 1 mM phenylmethylsulfonyl fluoride, and 1 mM leupeptin) at 4°C for 1 h. The cell lysates were centrifuged and the supernatants were collected. Concentration of protein in the supernatants was determined using bicinchoninic acid (BCA) assay (Thermo, Rockford, IL, USA).

Supernatants were denatured at 100°C for 5 min in 10% sodium dodecyl sulfate (SDS) sample buffer with 2% ß-mercaptoethanol, subjected to electrophoresis in SDS-PAGE gels (20 μg protein/lane), and transferred to nitrocellulose membrane (Schleicher & Schuell, Dassel, Germany). The membrane was cut into 3 pieces and blocked with PBS containing 4% low-fat milk (Yukijirushi, Co. Ltd., Hokkaido, Japan) for 1 h at RT. After 2 washes with PBS-Tween 0.05%, each membrane was probed overnight at 4°C, with one of the following monoclonal antibodies diluted in 1% BSA-PBS: (1) mouse monoclonal anti-human antibody (1E9) to scramblase 1 (abcam) (1.5 μg/ml); (2) mouse monoclonal anti-human antibody (1.5 μg/ml; Life Span Biosciences, Inc., Seattle, WA, USA); or (3) PLSCR1 monoclonal antibody (M12), clone 1E11, 1.0 μg/ml (Abnova, Taipei, Taiwan). After 2 washes, membranes were exposed to horseradish peroxidase-conjugated goat anti-mouse IgG antibody (1:5000; Jackson ImmunoResearch Laboratories, West Grove, PA, USA) in 1% BSA-PBS at RT for 1 h. Immunoreactive proteins were visualized using enhanced chemiluminescence assay (Amersham Biosciences, Piscataway, NJ, USA) and the optical imaging system (Multi Gauge ver. 3.0, LAS-4000 min, Fujifilm, Japan).

Measurement of cell-surface PS exposure. Cell-surface exposure of PS was evaluated by flow-cytometry using FACS Calibur (Becton Dickinson Immunocytometry Systems, San Jose, CA, USA) with the Cell Quest program. Monocytes were isolated, as described above, from the subjects who agreed to the double blood collection. Monocytes from 29 patients and 24 healthy subjects had double staining with Annexin-V-Fluos labeling kit (Roche Applied Science, Penzberg, Germany) and BD Pharmingen™ PE anti-human CD14 antibody (BD Bioscience Pharmingen, Franklin Lakes, NJ, USA) for 15 min at 4°C and exposed to FACS analysis. From each sample, data from 10,000 counted-gated viable cells were collected and data were expressed as the percentage of gated CD14+ cells, annexin V+ cells in the total gated cell population.

Statistical analysis. Statistical evaluation was performed by Student's t-test. Either Spearman's rank correlation coefficient or Pearson's correlation were used for analyzing the correlations as appropriate. The significance level was set at $p < 0.05$.

RESULTS

Plasma D-dimer levels. Thirty-three out of 60 SLE patients (55%) had elevated plasma D-dimer. Levels of D-dimer were significantly higher in SLE as compared with those in healthy subjects (1.3 ± 0.7 vs 0.6 ± 0.2 g/ml, respectively; $p < 0.0001$). There was no difference in plasma D-dimer levels between patients with APS and those without.

Antiphospholipid antibodies. aCL and anti-$ß_2$-GPI antibodies were found positive in 17% and 22% of the patients, respectively. Isotype distribution is shown in Table 1. Titers of aCL in positive samples ranged from 18.5 to 80 GPL for the IgG isotype, and 51 to 54 MPL for the IgM isotype. Among patients with positive anti-$ß_2$-GPI antibodies, titers ranged from 2.2 to 105 U/ml for the IgG isotype, and 8.4 to 40 U/ml for the IgM isotype. LAC was positive in 33% of the patients.

Expression of PLSCR1 mRNA in monocytes. RT-PCR was performed to amplify the full-coding sequence of PLSCR1 mRNA. Polyacrylamide gel showed that the PCR product of monocytes had 4 bands, of 1122 bp, 905 bp, 750 bp, and 551 bp (Figure 1). To compare the expression pattern of PLSCR1, total RNA samples from monocytes of 25 SLE patients (15 with APS) and 21 healthy controls were exam-

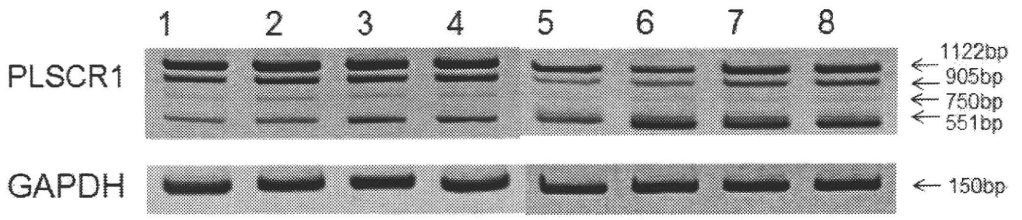

Figure 1. PLSCR1 RT-PCR in CD14+ cells from healthy controls and patients with systemic lupus erythematosus (SLE). RT-PCR products are resolved in 9% polyacrylamide gel. Bands correspond to PLSCR1 and GAPDH products of total RNA from 4 healthy individuals (lanes 1-4), 2 patients with SLE and antiphospholipid syndrome (APS) (lanes 5 and 6), and 2 patients with SLE without APS (lanes 7 and 8).

ined. The intensities of each splice variant differed among the individuals, but there was no specific pattern in the splice variant band intensity in patients with SLE. Because the variants did not turn to the protein, the biological significance of splice variants was not specified.

Sequencing analysis of PLSCR1 splice variants. One fragment of 1122 bp and a mixture of 905 bp, 750 bp, and 551 bp fragments were inserted into the pcDNA3.1 vector. Eighteen independent transformed cell clones were identified to have the expected inserts. DNA sequencing of these clones showed that 6 contained the 1122 bp DNA fragment corresponding to the complete coding sequence for PLSCR1 (GenBank accession NM_021105). Seven clones contained the 905 bp fragment and were identical to the PLSCR1 cDNA, except for a deletion of a 218 bp fragment corresponding to full exon 4 of PLSCR1 as revealed by the LI-COR AlignIR software. Three clones contained the 750 bp fragment and were identical to the PLSCR1 cDNA, except for the deletion of 2 fragments of 218 bp and 221 bp, which correspond to full exons 4 and 6 of PLSCR1, respectively. Two clones contained the 551 bp fragment and were identical to the PLSCR1 cDNA except for the deletion of 3 fragments of 218 bp, 221 bp, and 162 bp fragments corresponding to full exons 4, 6, and 7 of PLSCR1, respectively. Sequence homology searches with BLAST programs revealed that those sequences might be alternative splice variants of human PLSCR1 mRNA (Figure 2).

Western blotting for PLSCR1. Cell lysate products from IFN-activated PBMC of one healthy donor were assayed by Western blotting using 3 monoclonal antibodies directed to 3 different epitopes of PLSCR1. A single band at 37 kDa corresponding to full-length PLSCR1 was detected in IFN-activated cells (Figure 3).

Evaluation of full-length PLSCR1 mRNA levels by real-time PCR. Mean levels of full-length PLSCR1 mRNA were significantly higher in SLE patients than in controls (2.9 ± 1.5 vs 1.3 ± 0.4, respectively; $p < 0.00001$). PLSCR1 mRNA distribution is shown in Figure 4. No statistically significant correlations were found between levels of PLSCR1 mRNA expression and the titers of anti-DNA antibodies, IgG/M aCL, or IgG/M anti-$ß_2$-GPI antibodies. SLEDAI and CRP levels did not correlate significantly with levels of PLSCR1 expression.

Cell-surface PS expression on CD14+ cells. Flow-cytometric analysis showed that the amount of expressed PS on cell

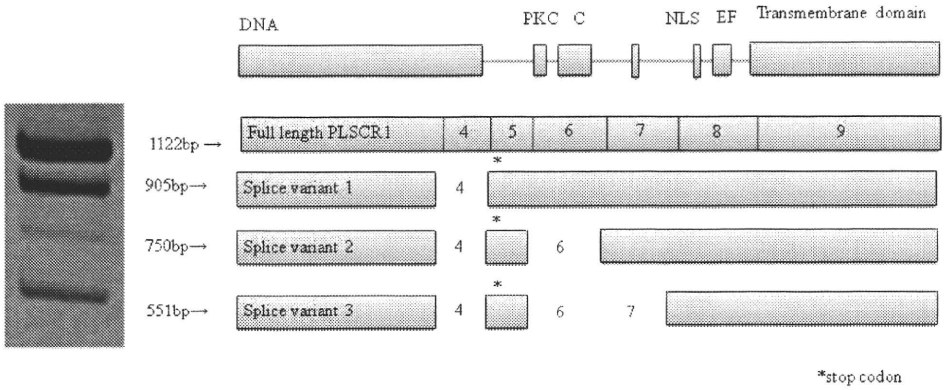

Figure 2. Human PLSCR1 mRNA isoforms. Top panel shows the exon structure and corresponding functional motifs of human PLSCR1 including the DNA binding domain (DNA), protein kinase C phosphorylation site (PKC), cystein-rich domain (C), nuclear localization signal (NLS), EF hands (EF), and transmembrane domain[32]. Exons are not drawn to scale. Lower panel shows human PLSCR1 products of total RNA from monocytes with exons at the right. Splice variants 1 to 3 highlighted in the right panel correspond to the 3 identified PLSCR1 variants. *Stop codon.

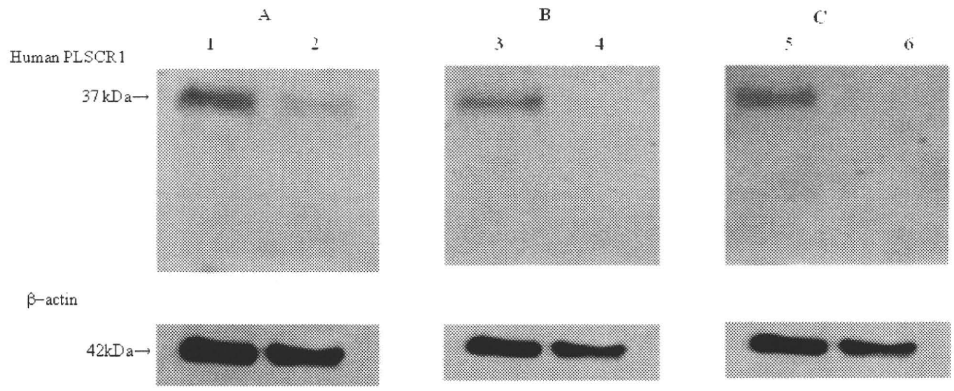

Figure 3. Western blotting shows cell lysates from peripheral blood mononuclear cells from a healthy control treated with (lanes 1, 3, and 5) or without interferon-α (IFN) (lanes 2, 4 and 6) for 24 hours. Western blotting was assayed using 3 monoclonal antibodies against human PLSCR1, (A) antibody specific for human PLSCR1 N-terminal region, (B) antibody directed against the C-terminal region of PLSCR1, and (C) antibody directed against full-length recombinant PLSCR 1 protein. A single band of 37 kDa was observed in IFN-treated cells. Lower panel shows bands corresponding to ß-actin.

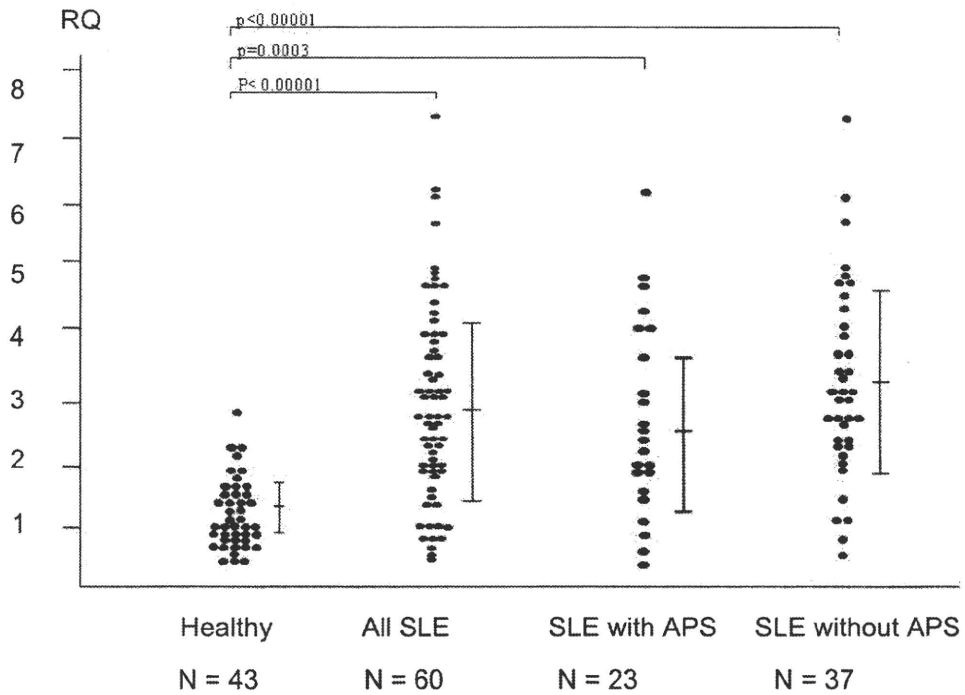

Figure 4. Quantitative real-time PCR analysis of PLSCR1. Gene expression of PLSCR1 in CD14+ cells was evaluated in healthy controls and in SLE patients with or without antiphospholipid syndrome (APS) by real-time PCR. Values were normalized to expression of the housekeeping gene GAPDH and expressed as relative quantification (RQ) in the Y-axis. Data are shown as individual results. Horizontal lines show the mean ± SD. PLSCR1 mRNA expression was significantly higher in patients with SLE.

surface was increased in CD14+ cells from SLE patients compared to controls (Table 2). No statistically significant correlations were found between the levels of PS expression and the autoantibodies investigated above or with SLEDAI/CRP levels.

In addition, no statistically significant correlation was observed between PLSCR1 mRNA levels and PS expression on CD14+ cells in patients with SLE.

DISCUSSION

In our study, we showed enhanced fibrin turnover in patients with SLE without acute thrombosis, presumably related to the prothrombotic tendency seen in such patients. A history of thrombosis was found in 23 SLE patients, which, together with increased fibrin turnover represented by elevated D-dimer plasma levels, is in concordance with the epidemiological observation of increased frequency of thrombotic events in SLE[3].

Table 2. Exposure of phosphatidylserine on the cell surface. Values are mean ± SD of percentage of annexin V high-binding cells.

Group		p
Healthy subjects, n = 24	17.8 ± 5.8	
SLE patients, n = 29	25.7 ± 11.6	1 vs 2, 0.003
2a APS, n = 7	20.6 ± 8.2	1 vs 2a, NS
2b non-APS, n = 22	27.3 ± 12.2	1 vs 2b, 0.003

SLE: systemic lupus erythematosus, APS: antiphospholipid syndrome. NS: not statistically significant.

Several studies show that SLE patients are at high risk of thromboembolic disease. The presence of aPL, other thrombotic risk factors, and predisposing conditions may contribute to the pathogenesis of the thrombophilic state in SLE, but the underlying disease mechanisms of the thrombotic tendency in SLE are not yet completely clarified[3,19,20,21,22,23].

Cell activation leads to rapid redistribution of cell membrane phospholipids and the appearance of PS on the cell surface. One of the main enzymes responsible for the externalization of PS is PLSCR1, and we speculate that SLE patients may have some abnormality in the regulation of PS expression by PLSCR1.

We investigated PLSCR1 mRNA expression in monocytes and identified 3 novel splice variants in PLSCR1, regardless of the presence of SLE. Human PLSCR1 gene is located on chromosome 3q23 and spans about 30 kb with 9 exons. Our sequencing analysis revealed 3 splicing variants generated through exon 4, exons 4/6, or exons 4/6/7 splicing out, respectively. Although these splice variants do not correspond to new isoforms of PLSCR1 protein, their identification is essential for accuracy in the quantification of PLSCR1 mRNA expression by PCR-based methods. Recently, Bernales, *et al*[24] evaluated the gene expression of PLSCR1 mRNA in PBMC from 12 SLE and 7 primary APS patients, and found higher expression of PLSCR1 mRNA in primary APS patients. We also analyzed PLSCR1 mRNA expression in monocytes from 17 primary APS patients (data not shown), and observed enhanced levels in SLE compared to those in primary APS patients. Moreover, the presence of APS in SLE patients did not affect PLSCR1 mRNA levels. The discrepancy in these data may be due to the different methodology used for PLSCR1 mRNA quantification, or to patient variables that may influence expression of PLSCR1. Bernales, *et al*[24] used a pair of primers that recognized the junction sequence between exons 1 and 2, leading to quantification of the full-length PLSCR and the 3 spliced mRNA variants. In contrast, our primer selection recognized the junction sequence between exons 3 and 4, resulting in quantification of full-length PLSCR1 mRNA expression only. Our RT-PCR results showed that the intensities of each splice variant differed among individuals, but there was no specific pattern in the band intensity in patients with SLE. Because the variants did not turn to the protein, the biological significance of splice variants was not specified. Therefore, we did not quantify the splice variants themselves.

In our study, SLE patients had elevated expression of PLSCR1 mRNA in circulating procoagulant cells, as well as high plasma levels of D-dimer in the absence of lupus activity and acute thrombosis, suggesting the prothrombotic state in SLE as a baseline. We had predicted a correlation between lupus activity and monocyte variables, but in fact SLEDAI scores did not correlate significantly with them. We consider that PLSCR1 upregulation is due to total biological alteration, which generally occurs in patients with SLE, but not to particular factors such as aPL.

PLSCR1 was reconstituted from platelets and erythrocytes[25,26], but has also been detected in a variety of cells[10]. Considering procoagulant cell activation in patients with SLE, it is likely that PLSCR1 overexpression in other procoagulant cells occurs in lupus patients.

PLSCR1 expression is induced by IFN[27], or by various growth factors[28,29,30]. Kirou, *et al*[31] showed that expression of IFN-α-inducible genes was significantly higher in PBMC from SLE than in those from controls, indicating IFN-α is the predominant stimulus for those inducible genes in SLE. Increased PLSCR1 expression may be related to IFN-α upregulation in SLE patients. Upregulation of IFN-α is considered to be linked to the inflammation and autoimmunity characteristic of SLE, and possibly being extended to thrombophilia through overexpression of PLSCR1. Our SLE patients had high fibrin turnover regardless of the presence of aPL. However, the thromboembolic complications in SLE are more common in patients with aPL, pointing to some regulator mechanisms that counterbalance the prothrombotic tendency. Antiphospholipid antibodies may affect those regulator mechanisms and represent an aggressive driver to promote thrombosis in SLE.

We demonstrated that PS exposure is relatively increased in the surface of monocytes in patients with SLE compared with healthy controls, but we failed to demonstrate the linear correlation between PLSCR1 mRNA levels and monocyte PS expression. The exposure of PS on monocytes is likely related to multiple mechanisms such as the inhibition of an ATP-dependent aminophospholipid translocase activity, an enzyme responsible for the maintenance of membrane phospholipid asymmetry in quiescent cells, and other processes required to maintain the integrity of the membrane. PLSCR1 is not the sole determinant of PS externalization and the balance between aminophospholipid translocase and PLSCR1 activities may ultimately determine the appearance of PS on the cell surface. PLSCR1 is, in any case, a strong driver of PS externalization.

We identified novel splice variants of PLSCR1. Monocytes in SLE patients had increased PLSCR1 mRNA expression, suggesting that PLSCR1 is one of the contributing factors in the prothrombotic tendency in SLE. Apart